A simple homogeneity test for estimates of dose obtained using OSL

Rex Galbraith
Department of Statistical Science, University College London, Gower Street, London WC1E 6BT, U.K.

(Received 2 January 2004; in final form 19 February 2004)

In optical dating (and in other dating methods) it is often required to compare age estimates, or equivalent dose estimates, for a number of single grains or aliquots. Typically each estimate has a different and (hopefully) known precision, which needs to be taken into account. A useful graphical method in this situation is the radial plot (Galbraith, 1988; Galbraith *et al.*, 1999) in which standardised estimates are plotted against the reciprocals of their standard errors. One feature of this plot is that a set of estimates that agree with each other, within error, will scatter homoscedastically, with unit standard deviation, about a line through the origin. This gives a visual assessment of which estimates are consistent with a common age or dose.

Often such a visual assessment will be sufficient, but sometimes it may be useful to assess more formally whether several estimates are consistent with a common value. This note points out that there are standard statistical tests available for this purpose.

Homogeneity test

Suppose that we have n independent estimates $z_1, z_2, \ldots, z_n$ with standard errors $\sigma_1, \sigma_2, \ldots, \sigma_n$. Let μ_i denote the expected value of z_i, so we can regard z_i as an observation from a distribution with mean μ_i and standard deviation σ_i. We wish to test the null hypothesis that $\mu_i = \mu$, a common (but unknown) value for each i.

There is a standard test based on the assumption that z_i is from a Normal distribution. In this case, the maximum likelihood estimate of μ (under the null hypothesis) is the weighted mean

$$\hat{\mu} = \frac{\sum_{i=1}^{n} w_i z_i}{\sum_{i=1}^{n} w_i} \quad \text{where} \quad w_i = \frac{1}{\sigma_i^2}$$

and the homogeneity test statistic is

$$G = \sum_{i=1}^{n} w_i (z_i - \hat{\mu})^2 .$$

If the μ_i are all equal, then G will be from a χ^2 distribution with $n-1$ degrees of freedom. If the μ_i differ then G will tend to be larger.

So the test is to calculate G and hence calculate the "P-value", which is the probability that a random value from the χ^2 distribution with $n-1$ degrees of freedom is greater than G. A significantly small P-value, with the usual conventions (e.g., less than 0.05 or 0.01), provides evidence that the μ_i are not all equal.

It is worth noting immediately that a significant P-value can also arise if the standard errors σ_i are not correct, particularly if they under-estimate of the true standard errors. This possibility should be borne in mind in practice. To put it another way, one is really assessing whether the observed variation in z_i is consistent with what would be expected from the given σ_i alone.

Relation with radial plots

The above test can be interpreted in terms of a radial plot, where $y_i = z_i/\sigma_i$ is plotted against $x_i = 1/\sigma_i$. The estimate of μ can be written equivalently as

$$\hat{\mu} = \frac{\sum_{i=1}^{n} x_i y_i}{\sum_{i=1}^{n} x_i^2}$$

which is the slope of the ordinary least squares regression line through the origin; and G can be written as

$$G = \sum_{i=1}^{n} (y_i - \hat{\mu} x_i)^2$$

which is the sum of squared residuals about the regression line. In effect, the test is assessing whether the residual standard deviation about the regression line through the origin is consistent with 1. In practice, in a radial plot one normally uses $y_i = (z_i - z_0)/\sigma_i$ for some convenient z_0, but the above interpretation still applies.

Application to OSL doses

Many optical dating methods use a single aliquot regenerative dose (SAR) protocol, which produces a dose estimate and its standard error for each grain or aliquot in a sample. Suppose we wish to assess whether these estimates are consistent with a common value. There is more than one way to apply the above test. For example, we could let z_i be the dose estimate (in Gy), or we could let z_i be the natural *log* of the dose estimate. Because the test assumes that z_i is from a Normal distribution, the latter choice may often be preferred. In this case, σ_i would be the standard error of the log dose — which is effectively the *relative* standard error of the dose. Note furthermore that the standard error of a dose estimate generally increases with the size of the dose, whereas the relative standard error does not (to the same extent, at least). This is another reason why using the log doses may be preferred.

For illustration, consider the data in Table 1, taken from Galbraith *et al.* (1999). These are palaeodose estimates and standard errors (in Gy), and the corresponding log palaeodose estimates and their standard errors, for seven single grains of quartz.

Grain number	Palaeodose (Gy)			Log palaeodose	
	estimate	s.e.		estimate	s.e.
19	30.1	4.8		3.4055	0.1607
22	53.8	7.1		3.9857	0.1314
25	54.3	6.8		3.9943	0.1253
50	29.0	4.3		3.3663	0.1494
99	47.6	5.2		3.8630	0.1087
105	44.2	5.9		3.7887	0.1330
107	43.1	3.0		3.7627	0.0702

Table 1.
Data for example calculation

In this example it is more reasonable to apply the test to the log palaeodose estimates. Indeed, the standard errors of these were obtained directly from the OSL photon counts, while the standard errors of the palaeodoses were derived from them — e.g., for grain 19, as $30.1 \times 0.1607 = 4.8$.

The reader may verify that, from the above formulae, $\hat{\mu} = 3.7737$ and $G = 19.10$, with 6 degrees of freedom. Hence the P-value is approximately 0.004 (the probability that a value from $\chi^2(6)$ is greater than 19.10), which is strong evidence against the null hypothesis. On this basis there is strong evidence that the estimated doses are not consistent with a common value, within the given errors. As noted above, this may be because the true doses vary or because the standard errors have been under-estimated (or both).

Figure 1 shows a radial plot of the data in Table 1 which suggests visually that the estimates are slightly over-dispersed — for example, two of the seven points scatter outside the ± 2 standard error band shown. This plot uses $z_0 = \hat{\mu} = 3.7737$, so the horizontal radius corresponds to $e^{3.7737} = 43.5$ Gy.

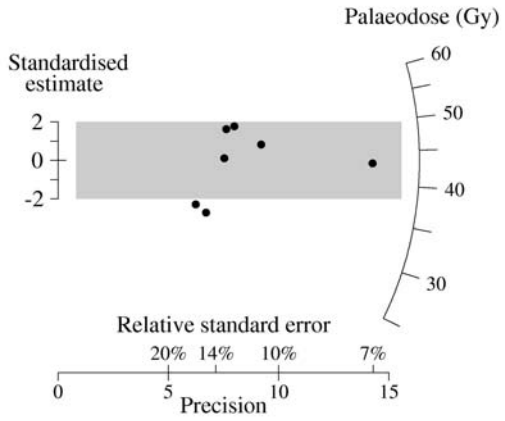

Figure 1.
Radial plot (log scale) of the palaeodose estimates in Table 1.

Galbraith *et al.* (1999) used these data to illustrate the calculations for the central age model. The over-dispersion parameter σ was estimated to be 0.1724, with standard error 0.0694, suggesting, in particular, that σ is greater than zero (rather than equal to zero). That is, the dose estimates vary by more than their standard errors would imply, in agreement with the above test. The central age model, in addition, gives an estimate of the amount of over-dispersion (albeit rather an imprecise one in this example with only seven grains).

Further remarks

Homogeneity tests, such as that above, have been found useful in other contexts — for example in fission track dating and in "meta analysis" of medical trials. When over-dispersion is present, different types of question may then arise as to its cause and effect, which may invite different types of subsequent

analysis. A good modern reference to the above test is Armitage *et al*, (2002), pages 216 and 643. This is a new edition of a classic book aimed at medical researchers, but it is also an excellent general reference for modern statistical methods.

The above test has quite low power, particularly when n is large and the μ_i do not vary greatly. That is, moderate heterogeneity of the μ_i may not produce a significantly large G. This may not be a bad thing in the present context. As always, it should be remembered that data may be consistent with the null hypothesis and at the same time be consistent with other hypotheses.

Finally, the fact that standard errors of dose estimates tend to increase with the size of dose, has other implications. For example, when plotting a number of dose estimates in a histogram, the larger ones will tend to scatter more. This is one reason why such histograms are often positively skewed.

I thank Geoff Duller and Bert Roberts for useful comments.

References

Armitage, P., Berry, G., and Mathews J.N.S. (2002) *Statistical Methods in Medical Research*, 4th Edition, Blackwell, 2002.

Galbraith, R.F., (1988) Graphical display of estimates having differing standard errors. *Technometrics*, 30**,** 271–281.

Galbraith, R.F., Roberts, R.G., Laslett, G.M., Yoshida, H. and Olley, J.M. (1999) Optical dating of single and multiple grains of quartz from Jinmium rock shelter, Northern Australia: Part I, Experimental design and statistical models. *Archaeometry*, 41**,** 338–364.

Reviewer

Geoff Duller

Gamma dosing and shielding of a human tooth by a mandible and skull cap: Monte Carlo simulations and implications for the accuracy of ESR dating of tooth enamel

Roger Nathan[1] and Rainer Grün[2,3]
[1]Research Laboratory for Archaeology and the History of Art, University of Oxford
6 Keble Road, Oxford OX1 3QJ, UK

[2]Research School of Earth Sciences; [3]Research School of Pacific and Asian Studies
The Australian National University, Canberra ACT 0200, Australia

(Received 28 January 2004; in final form 10 May 2004)

Introduction

In recent years, ESR analysis has been used for the direct dating of human tooth enamel (e.g. Thorne et al. 1999, Grün et al. 2003). During the refereeing process of a paper on the ESR dating of an enamel fragment from Skhul, the dating results were objected to because of the unknown dose rate contributions to the tooth from the human mandible and the skull cap, which are in close proximity to the sample. Here we address the problem of dosing and shielding of a human tooth by a mandible and skull cap, and present model calculations for three cases: Skhul, Mungo and Border Cave.

Skull radiation modelling

Dosimetry was modelled using the Monte Carlo radiation transport code MCNP4C (Briesmeister 2000). Input files are employed which contain: a) spatially-resolved materials; b) radiation emission spectra and source locations; c) radiation detector tallies; and d) additional systemic information. MCNP follows the history of each gamma source photon (and any secondary particles generated) by stochastically sampling initially a starting position, direction and energy and then interactions based on tabulated data. Secondary electrons were assumed to be deposited locally. The strength of Monte Carlo methods arises from their ability to calculate radiation transport in complex environments with little increase in systematic uncertainties.

To assess the dose rate contributions of a mandible and a skull cap, we used a computer tomography scan (axial slices) of the Skhul V specimen (see home site of the Peabody Museum, Harvard University) as the basis for the geometry. The data were re-sampled to yield voxels (short for *volume pixel*, the smallest distinguishable box-shaped part of a three-dimensional image) of approximately 4mm isotropic dimension. Further processing was needed to insert the skull geometry into the Monte Carlo model. We designed a program to divide up the skull and surrounding sediment into several thousand "cells" optimised for computational efficiency. The calculations were carried out for "typical" dry sediment (Garrels and MacKenzie 1971) as 1.775 g cm^{-3} and "typical" wet sediment of 2 g cm^{-3} with water present 25% by weight following Aitken (1985). During the life time of an individual, the average density of dense human bone sections is around 1.9 g cm^{-3} (Cameron et al. 1999, p. 96). During diagenesis, bones may either lose mineral component, i.e. become less dense, or continue to mineralise, i.e. become more dense (Hedges 2002). Calculations were carried out for densities of 1.6 g cm^{-3} and 2.7 g cm^{-3} to cover the possible density range of fossil bones. To calculate the overall dose rates to a tooth from the mandible and skull cap, it is important to know how much of the sediment dose rate from Th and K is shielded. These values were also calculated for the above conditions.

The gamma spectra were downloaded 21 April 2003 from the Evaluated Nuclear Structure Data File (ENSDF) database at the Brookhaven National Laboratory http://www.nndc.bnl.gov. All models were run for approximately 20 million photon histories. MCNP provides energy deposition in detectors normalised to one source particle. The infinite matrix dose (IMD) for each decay group was estimated by determining the energy deposited in a known mass embedded inside a large volume of uniform fossil material. The ratio of tooth self-dose to IMD self-dose, Ψ, can be written:

$$\Psi = \frac{D_{tooth}}{D_{IMD}} \frac{m_{skull}}{m_{tooth}} \frac{m_{IMD\ detector}}{m_{IMD\ volume}} \quad (1)$$

where D is the energy deposited and m is the mass. In an infinite matrix, there exists a state of "radiation equilibrium", such that energy entering a small mass is equal to the energy exiting. In this case, 1-Ψ provides a measure of the attenuation of the IMD within the tooth. Although this is not strictly the case for the models used here, the composition of sediment (average Z-value) is sufficiently similar to the composition of the skull to warrant this approximation and the uncertainties in the attenuation estimates are incorporated in the results (see e.g. gamma attenuation factors of Hubbell 1982).

Results of the modelling

The gamma dose contributions are tabulated in Tables 1a-c (ρ = 1.6 g cm^{-3}) and 2a-c (ρ = 2.7 g cm^{-3}) as fractions of the bone IMD. Uncertainties are associated with counting statistics of the model.

The most obvious and somewhat surprising result is that the IMD fraction of the complete skull to a specific tooth (Tables 1a and 2a) is not simply the sum of the skull cap (Tables 1b and 2b) and mandible (Tables 1c and 2c). This is caused for a tooth in the mandible (i) by the greater distance to the skull cap compared to a tooth in the upper jaw, and (ii) by partial shielding of the dose rate from the skull cap by the teeth in the upper jaw. The equivalent symmetrical relationships apply to a tooth in the upper jaw. The self-dosing/shielding of a row of four teeth is in the range of 5% of the IMD.

For the U-chains in equilibrium, the wetness of the sediment has virtually no influence on dose rate calculations. The fractions of the whole skull's (ρ = 1.6 g cm^{-3}) uranium IMD received by a lower incisor are 0.0731 (dry sediment) and 0.0737 (wet sediment, see Table 1a), i.e. the differences are less than 1%.

The contribution of the skull to the dose rate of a tooth is strongly dependent on the density of the skull (compare Tables 1 and 2). The percentages of the whole skull's uranium IMD received by a lower incisor are 0.0731 (ρ = 1.6 g cm^{-3}, dry sediment) and 0.1137 % (ρ = 2.7 g cm^{-3}, dry sediment), the latter being about 56% higher.

To calculate the effect of gamma dosing from the mandible and skull cap, two processes have to be considered:

1) U-series disequilibrium. About 93% of the total gamma dose rate from the U-decay chains are generated by the decay of ^{214}Pb and ^{214}Bi. Therefore, the ^{230}Th/^{238}U ratio has to be considered for dose rate calculations.

The activity of ^{230}Th is expressed by:

$$^{230}Th = {}^{234}U(1-e^{(-\lambda_{230}t)}) = {}^{238}U(1-e^{(-\lambda_{230}t)})$$

$$if\ \frac{^{234}U}{^{238}U} = 1 \quad (2)$$

where λ_{230} is the decay constant of ^{230}Th. Equation (2) requires that ^{234}U and ^{238}U are in secular equilibrium at t=0 (i.e. when the uranium is incorporated into the sample). This is usually not the case because most natural waters have an excess of ^{234}U over ^{238}U (e.g. Chapter V in Cherdyntsev 1971). This is due to the fact that ^{234}U is produced by -decay of ^{238}U: when an alpha particle is emitted, the decaying atom recoils, leading to a weakening of its lattice position. Dissolution of minerals starts preferentially at weakened lattice sites, as a consequence, these solutions are enriched with ^{234}U. Alternatively, the recoiled atom can be directly ejected from the mineral surface into the solution. Because of its long half-life of about 244 ka, the excess ^{234}U activity has to be taken into account:

$$\frac{^{230}Th}{^{238}U} = (1-e^{(-\lambda_{230}t)}) + \frac{\lambda_{230}}{\lambda_{230}-\lambda_{234}}(\frac{^{234}U}{^{238}U}-1)(1-e^{-(\lambda_{230}-\lambda_{234})t}) \quad (3)$$

where λ_{234} is the decay constant of ^{234}U.

2) U-uptake. Most bones and teeth experience U-uptake after burial, and this has a strong influence on dose rate calculations (e.g. Grün 1989). To simplify calculations, it is convenient to calculate the dose a tooth has received from a bone that represents a closed system for U-series (i.e. applying the CSUS-ESR model of Grün 2000), rather than iteratively evaluating average dose rates using the p-value system (Grün et al. 1988). This has the advantage that the dose calculation becomes independent of the actual age of the sample. The differences between

CSUS-ESR and open system p-value dose calculations are small (see Grün 2000).

We now present the gamma dose calculations for three cases:
1) Skhul II (Grün et al., in preparation)
2) Mungo 3 (Thorne et al. 1999) and
3) Border Cave 5 (Grün et al., 2003)

Skhul II (partial mandible, partial skull): To calculate the possible effects of U-dosing of the skull and shielding of sediment gamma dose by the skull, the two extreme $^{230}Th/^{238}U$ values can be used, that of the dentine of the tooth from Skhul II (Model 1) and the surface layer of a bone from Skhul IX (Model 2). Skhul II consist only of a partial mandible and fragments of the skull (Garrod and Bate 1937, p. 98), therefore, the overall effect of dosing will be smaller than calculated for a whole mandible and skull cap.

Model 1: U-series data were evaluated on the dentine: U(DE) = 60 ppm; $^{234}U/^{238}U = 1.073 \pm 0.003$; $^{230}Th/^{238}U = 0.275 \pm 0.006$, resulting in a closed system U-series age of 32.1 ± 0.8 ka and an initial $^{234}U/^{238}U$ value of 1.080 ± 0.003. The time-averaged $^{230}Th/^{238}U$ ratio is 0.144 and the $^{231}Pa/^{235}U$ ratio is 0.274. The average $^{234}U/^{238}U$ ratio does not have to be considered as the gamma intensities of ^{234}U are very small. Assuming that the U-series data apply to the whole skull, using the values from Tables 1a and 2a and the dose rate values of Adamiec and Aitken (1998), total dry gamma doses of 3.73 Gy (ρ = 1.6 g cm^{-3}) and 5.59 Gy (ρ = 2.7 g cm^{-3}) are obtained.

At the same time, the tooth is shielded by the skull and mandible from the sediment gamma dose rate generated by the radioactive isotopes in the sediment, namely the U and Th decay chains in equilibrium and K. The average composition of the sediment at Skhul is 2.00 ± 0.68 ppm U, 2.38 ± 1.4 ppm Th and 0.45 ± 0.15% K. The total shielded sediment gamma dose in 32.1 ka is 1.22 ± 0.30 Gy (ρ = 1.6 g cm^{-3}) and 1.90 ± 0.48 Gy (ρ = 2.7 g cm^{-3}). Assuming an age of about 120 ka, the shielded doses are 4.56 ± 1.12 and 7.10 ± 1.79 Gy for ρ = 1.6 g cm^{-3} and 2.7 g cm^{-3}, respectively. The net effect of the presence of the skull would lead to corrections of less than 1.6 Gy, or less than 1.6% on a measured dose value of 98.7 ± 7.8 Gy.

Model 2: A bone surface sample from Skhul IX yielded the highest closed system U-series age with 8.7 ppm U, $^{234}U/^{238}U = 1.052 \pm 0.002$; $^{230}Th/^{238}U = 0.742 \pm 0.006$, resulting in a closed system U-series age of 131 ± 2 ka and an initial $^{234}U/^{238}U$ value of 1.075 ± 0.002. The time-averaged $^{230}Th/^{238}U$ ratio is 0.446 and the $^{231}Pa/^{235}U$ ratio is 0.662. Using the same procedures as above, we obtain total U-doses of 5.55 and 8.53 Gy for densities of 1.6 and 2.7 g cm^{-3}, respectively. The total shielded gamma doses over 131 ka are 4.98 ± 1.22 and 7.75 ± 1.95 Gy for densities of 1.6 and 2.7 g cm^{-3}, respectively, requiring net dose corrections of less than 0.8 Gy.

As mentioned above, because of the fragmentary nature of the mandible and skull, the overall effect on a tooth from Skhul II is most probably much less than 1.6 Gy (the higher correction value derived from model 1).

Mungo 3 (mandible and skull cap): The average U-concentration in the bone material is 5.5 ± .9 ppm, $^{234}U/^{238}U = 1.319 \pm 0.035$ (average of TIMS measurements on bones); $^{230}Th/^{238}U = 0.610 \pm 0.067$ (average of TIMS and gamma spectrometric measurements of the bones and skull), resulting in a closed system U-series age of 65.6 ± 10 ka and an initial $^{234}U/^{238}U$ value of 1.384 ± 0.035. The time averaged $^{230}Th/^{238}U$ ratio is 0.339 and the $^{231}Pa/^{235}U$ ratio is 0.461. This results in a gamma dose from the skull (over the time period of 65.6 ka) of 1.38 and 2.11 Gy for densities of 1.6 and 2.7 g cm^{-3}, respectively. The average composition of the Mungo sediment is 0.27 ± 0.05 ppm U, 0.82 ± 0.04 ppm Th and 0.15 ± 0.01% K. The shielded doses for the same time are 0.57 ± 0.16 and 0.90 ± 0.5 Gy for densities of 1.6 and 2.7 g cm^{-3}, respectively, necessitating corrections of less than 1.21 Gy, or about 4.5% on a measured dose value of 26 ± 2 Gy (the mean EU age would be reduced from 63 to 60 ka). This is smaller than the quoted uncertainty of 6 ka for this age determination (Thorne et al. 1999).

Border Cave 5 (mandible only). The age of the sample has been estimated as 74 ka. The U-concentrations in bones in Border Cave are very low, in the range of 0.2 ppm resulting in a dose rate value from the mandible of less than 1 μGy a^{-1}. A sediment sample in the vicinity of the mandible had a composition of 2.05 ± 0.50 ppm U, 10.8 ± 0.2 ppm Th and 2.87 ± 0.10 % K. The mandible shields about 70 μGy a^{-1} for ρ = 1.6 g cm^{-3}. The bones from Border Cave are not mineralised so that calculations for ρ = 2.7 g cm^{-3} would be misleading. As a result, the total dose rate of 2026 μGy a^{-1} would decrease by 3.5 % and the age of the tooth would increase from about 74 to 77 ka.

Summary

We have calculated the overall effect of uranium gamma dosing and U, Th, and K shielding of the environmental dose rate by a human skull on the total

	Sediment type	^{238}U-^{234}Th	^{230}Th-^{206}Pb	^{235}U-^{231}Th	^{231}Pa-^{207}Pb	U	Th	K
IMD (μGy a^{-1} per ppm U, Th; %K)		2.0	109.0	0.5	1.4	113	48	243
Lower incisor	Dry	0.1657 ± 0.0017	0.0696 ± 0.0009	0.2536 ± 0.0013	0.1502 ± 0.0010	0.0731 ± 0.0009	0.0685 ± 0.0013	0.0605 ± 0.0009
	Wet	0.1689 ± 0.0017	0.0701 ± 0.0008	0.2560 ± 0.0013	0.1533 ± 0.0010	0.0737 ± 0.0008	0.0690 ± 0.0012	0.0611 ± 0.0012
Upper incisor	Dry	0.1645 ± 0.0021	0.0699 ± 0.0011	0.2518 ± 0.0017	0.1492 ± 0.0013	0.0734 ± 0.0011	0.0659 ± 0.0016	0.0606 ± 0.0012
	Wet	0.1669 ± 0.0021	0.0699 ± 0.0011	0.2570 ± 0.0017	0.1535 ± 0.0013	0.0735 ± 0.0011	0.0661 ± 0.0011	0.0612 ± 0.0010
Lower molar	Dry	0.1917 ± 0.0011	0.0858 ± 0.0006	0.2817 ± 0.0009	0.1788 ± 0.0007	0.0897± 0.0006	0.0839 ± 0.0009	0.0738 ± 0.0006
	Wet	0.1948 ± 0.0011	0.0861 ± 0.0006	0.2850 ± 0.0009	0.1829 ± 0.0007	0.0901 ± 0.0006	0.0844 ± 0.0006	0.0743 ± 0.0008
Upper molar	Dry	0.1912 ± 0.0014	0.0860 ± 0.0007	0.2796 ± 0.0011	0.1784 ± 0.0008	0.0899 ± 0.0007	0.0831 ± 0.0011	0.0749 ± 0.0008
	Wet	0.1947 ± 0.0014	0.0866 ± 0.0007	0.2846 ± 0.0011	0.1831 ± 0.0008	0.0906 ± 0.0007	0.0838 ± 0.0015	0.0755 ± 0.0009

Table 1a: Gamma dose contribution (columns 2-5) and gamma shielding (columns 6-8, U and Th chains in equilibrium) of a **whole skull** as percentage of the infinite matrix dose, IMD (**skull density 1.6 g cm^{-3}**)

	Sediment type	^{238}U-^{234}Th	^{230}Th-^{206}Pb	^{235}U-^{231}Th	^{231}Pa-^{207}Pb	U	Th	K
Upper incisor	Dry	0.1457 ± 0.0019	0.0591 ± 0.0010	0.2327 ± 0.0015	0.1294 ± 0.0011	0.0623 ± 0.0010	0.0573 ± 0.0015	0.0494 ± 0.0010
Upper molar	Dry	0.1618 ± 0.0011	0.0676 ± 0.0006	0.2512 ± 0.0009	0.1474 ± 0.0007	0.0711 ± 0.0006	0.0645 ± 0.0009	0.0584 ± 0.0006

Table 1b: same as Table 1a for the **skull cap.**

	Sediment type	^{238}U-^{234}Th	^{230}Th-^{206}Pb	^{235}U-^{231}Th	^{231}Pa-^{207}Pb	U	Th	K
Lower incisor	Dry	0.1309 ± 0.0004	0.0444 ± 0.0002	0.2163 ± 0.0004	0.1122 ± 0.0003	0.0475 ± 0.0002	0.0425 ± 0.0034	0.0374 ± 0.0024
Lower molar	Dry	0.1454 ± 0.0003	0.0517 ± 0.0001	0.2303 ± 0.0002	0.1255 ± 0.0002	0.0551 ± 0.0001	0.0497 ± 0.0022	0.0441 ± 0.0016

Table 1c: same as Table 1a for the **mandible**.

	Sediment type	^{238}U-^{234}Th	^{230}Th-^{206}Pb	^{235}U-^{231}Th	^{231}Pa-^{207}Pb	U	Th	K
Lower incisor	Dry	0.2211 ± 0.0021	0.1096 ± 0.0011	0.3111 ± 0.0016	0.2105 ± 0.0012	0.1137 ± 0.0011	0.1076 ± 0.0013	0.0951 ± 0.0008
Upper incisor	Dry	0.2164 ± 0.0026	0.1106 ± 0.0014	0.3072 ± 0.0020	0.2053 ± 0.0016	0.1145 ± 0.0014	0.1038 ± 0.0014	0.0949 ± 0.0011
Lower molar	Dry	0.2589 ± 0.0014	0.1347 ± 0.0007	0.3496 ± 0.0010	0.2509 ± 0.0008	0.1393 ± 0.0007	0.1313 ± 0.0010	0.1157 ± 0.0007
Upper molar	Dry	0.2571 ± 0.0014	0.1364 ± 0.0007	0.3479 ± 0.0011	0.2475 ± 0.0008	0.1409 ± 0.0007	0.1307 ± 0.0013	0.1179 ± 0.0012

Table 2a: Gamma dose contribution (columns 2-5) and gamma shielding (columns 6-8, U and Th chains in equilibrium) of a **whole skull** as percentage of the infinite matrix dose, IMD (**skull density 2.7 g cm^{-3}**)

	Sediment type	^{238}U-^{234}Th	^{230}Th-^{206}Pb	^{235}U-^{231}Th	^{231}Pa-^{207}Pb	U	Th	K
Upper incisor	Dry	0.1901 ± 0.0023	0.0912 ± 0.0012	0.2790 ± 0.0018	0.1769 ± 0.0013	0.0948 ± 0.0012	0.0885 ± 0.0015	0.0757 ± 0.0015
Upper molar	Dry	0.2145 ± 0.0014	0.1065 ± 0.0008	0.3036 ± 0.0011	0.2003 ± 0.0008	0.1105 ± 0.0008	0.0990 ± 0.0006	0.0902 ± 0.0011

Table 2b: same as Table 2a for the **skull cap**.

	Sediment type	^{238}U-^{234}Th	^{230}Th-^{206}Pb	^{235}U-^{231}Th	^{231}Pa-^{207}Pb	U	Th	K
Lower incisor	Dry	0.1728 ± 0.0006	0.0707 ± 0.0003	0.2581 ± 0.0004	0.1539 ± 0.0003	0.0744 ± 0.0003	0.0687 ± 0.0033	0.0594 ± 0.0021
Lower molar	Dry	0.1953 ± 0.0004	0.0832 ± 0.0002	0.2779 ± 0.0003	0.1756 ± 0.0002	0.0872 ± 0.0002	0.0798 ± 0.0025	0.0702 ± 0.0021

Table 2c: same as Table 2a for the **mandible**.

dose rate received by a tooth. The presence of bones near a tooth used for ESR dating may influence the resulting age estimate either way, depending on the relative balance between uranin in the bones and radioactive elements on the surrounding sediment, the ages may either increase or decrease (see calculated examples above). As it happens, the net effect is small for the three real cases presented in this study (< 5%). The average uranium dose rate from a whole cap is between about 7 and 14% of the skull's IMD (ρ = 1.6 g cm^{-3} and 2.7 g cm^{-3}). The average shielding of the total environmental dose rate by a complete skull is between about 7 and 12% (ρ = 1.6 g cm^{-3} and 2.7 g cm^{-3}). The effect of the presence of a skull is maximised in cases such as Border Cave, where the sediment dose rate is high and the uranium concentrations in the bones is very low. In other environments, the effect of increased U-concentrations in the bones of the skull (which are usually free of Th and K) is offset by (i) disequilibrium of the U-decay chains in the bones, (ii) delayed U-uptake by the bones, and (iii) shielding of the U, Th and K dose rates from the sediment.

It may be worth mentioning that when applying Tables 1 and 2, the true errors of any calculation will be rather large, as the dose rates are critically dependent on the precise position of the mandible and skull cap relative to the tooth. In most cases, the mandible and skull cap will have separated to some extent and parts of the bones may be missing (e.g. Skhul II). Nevertheless, it is useful to calculate the overall effect of dosing and shielding to estimate the magnitude of possible systematic errors.

Acknowledgment
This study was thankfully brought about by a tenacious referee who thought to have discovered a major source of uncertainty in the calculation of dose rates for human tooth enamel.

References

Adamiec, G. and Aitken, M.J. (1998). Dose-rate conversion factors: update. *Ancient TL* **16**, 37-50.

Aitken, M.J. (1985) *Thermoluminescence Dating*. Academic Press, New York.

Briesmeister, J.F. (2000) MCNP - A General Monte Carlo N-Particle Transport Code Version 4C. Report LA-13709-M, Los Alamos National Laboratory, USA.

Cherdyntsev, V.V. (1971) *Uranium-234*. Israel Program for Scientific Translations, Jerusalem.

Cameron, J.R., Skofronick, J.G. and Grant, RM. (1999). Physics of the Body. 2nd Ed., Medical Physics Publishing, Madison, WI.

Garrels, R.M., and MacKenzie, F.T. (1971) Evolution of sedimentary rocks. Norton, NY.

Garrod, D. and Bate, D. (1937) *The Stone Age of Mount Carmel. Vol. 1*, Oxford University Press, Oxford.

Grün, R. (1989) Electron spin resonance (ESR) dating. *Quaternary International* **1**, 65-109.

Grün, R. (2000) An alternative model for open system U-series/ESR age calculations: (closed system U-series)-ESR, CSUS-ESR. *Ancient TL* **18**: 1-4.

Grün, R., Beaumont, P., Tobias, P.V. and Eggins, S. (2003) On the age of Border Cave 5 human mandible. *Journal of human Evolution* **45**: 155-167.

Grün, R., Schwarcz, H.P. and Chadam, J.M. (1988) ESR dating of tooth enamel: Coupled correction for U-uptake and U-series disequilibrium. *Nuclear Tracks and Radiation Measurements* **14**: 237-241.

Grün, R., Stringer, C.B., Pike, A.W.G., McDermott, F., Nathan, R., Porat, N., Robertson, S., Taylor, L., Mortimer, G., Eggins, S., and McCulloch, M. (in preparation). Dating the human burials from Skhul.

Hedges, R.E.M (2002) Bone diagenesis: An overview of processes. *Archaeometry* **44**: 319-328.

Hubbell, J.H. (1982) Photo Mass Attenuation and Energy-absorption Coefficients from 1 keV to 20 MeV. *Applied Radiation and Isotopes* **33**: 1269-1290.

Thorne, A., Grün, R., Mortimer, G., Spooner, N.A., Simpson, J.J., McCulloch, M.T., Taylor, L. and Curnoe, D. (1999) Australia's oldest human remains: age of the Lake Mungo 3 skeleton. *Journal of Human Evolution* **36**: 591-612.

Reviewer
Bert Roberts

Preferable use of red-thermoluminescence (RTL)-dating for quartz extracts from archaeologically burnt pottery -comparison of RTL and BTL (blue-TL) measurements using single-aliquot regenerative-dose (SAR) method

[1]Tetsuo Hashimoto, [2]Takashi Yawata. and [2]Masato Takano

1. Department of Chemistry, Faculty of Science, Niigata University, Niigata, 950-2181, Japan
2. Graduate School of Science and Technology, Niigata University, Niigata, 950-2181, Japan
Corresponding Author: thashi@curie.sc.niigata-u.ac.jp

(Received 22 April 2004; in final form 15 May 2004)

Abstract

Red- (RTL) and blue-thermoluminescence (BTL) dating procedures for quartz aliquots were applied to nine Jomon pottery pieces, which were manufactured and used 3,500-6,000 years ago. Quartz grain extracts from each piece were measured with respects of both RTL and BTL using a new automated luminescence measuring system that included a small X-ray irradiator and a single-aliquot regenerative-dose (SAR) protocol. Equivalent doses from RTL were evaluated to be higher than BTL-doses in most cases. This is due to contamination of feldspar grains and/or to light-bleaching effects. In a few cases, BTL-quartz constituents have not been detected. The TL-age results, obtained using the equivalent doses and annual doses, indicated that the RTL-ages are closer to the predicted archeological ages, giving more reliable results than the BTL-ages. Conclusively, the RTL-dating was recommended for the quartz extracts from the archaeologically burnt materials in the present experiments, probably because of the high impurity contents in the quartz grains. Although the existing BTL-dating could be already applied to the pure quartz grains without much content of impurities, the check of TL-properties, including RTL or BTL, should be considered prior to the practical TL-dating for burnt quartz fractions.

1 Introduction

The blue-thermoluminescence (BTL) from quartz grains has been utilized for the TL-dating before the availability of highly sensitive TL-spectrometry and photographic observation (Aitken, 1985). In the beginning of the 1980s, the red-thermoluminescence (RTL) phenomena have been discovered in addition to the already well-known BTL phenomena within quartz grains of the Niigata dune sand after either natural or artificial exposure of radiation (Hashimoto et al., 1986). Subsequently, both the volcanically originating quartz grains and the artificially burnt ones were found to offer such RTL properties. Especially, in both the volcanically originating and the burnt quartz fractions, RTL measurements are preferable for dating over a period of 1 Ma (Hashimoto et al., 1987, 1993, 1999; Miallier et al., 1994). The causes of the RTL have been investigated by artificial thermal annealing treatments on some natural quartz crystals and by synthesizing quartz glasses with various kinds of impurities along with the aids of the sol-gel method of silica glass (Hashimoto et al., 1991, 1997). As a result, the rapid cooling process after annealing beyond 867^{o}C (β-quartz/tridymite phase inversion temperature) was found to be responsible for the RTL properties as well as the collaboration with the Al-impurity content beyond 100 ppm (Hashimoto et al., 1994, 1996).

In order to evaluate reliable paleo-doses or equivalent doses, a single-aliquot regenerative-dose (SAR) technique has been developed mainly for the optically stimulated luminescence (OSL) measurements, in which luminescence-measurement and irradiation could be repeatedly adopted under the same geometrical conditions (Wintle and Murray, 2000).

In this study, the RTL and BTL methods were applied to the evaluation of naturally accumulated doses (or paleo-doses) for the quartz extracts from pottery pieces. The SAR-protocol was employed using a new automated luminescence measuring system equipped with a small X-ray irradiator (Hashimoto et al., 2002a,b). The both RTL- and BTL-ages were determined from the relationship between the paleo-doses and the annual doses, which were estimated from the natural radioactivity of the ambient soil of the buried pottery pieces and crushed pottery material. The results were compared to each other as well as with the ages predicted from the mode of pottery and the stratigraphic viewpoints.

2 Experimental

2-1 Sample pieces of pottery

Pottery pieces from the Okumiomote site, situated in the northern district of Niigata, Japan, were used in this study. Nine pottery pieces were collected, together with related soil samples from four ruin sites: Achiyadaira, Shimozori, Miyasori, and Motoyashiki areas. From the archaeological view, the pottery samples were assumed to be manufactured and used about 3,500-6,000 years ago. During these periods, almost all pottery surfaces were decorated with some rope-shaped patterns, so that we called them Joumon (rope-pattern decorated) pottery. Soil samples of the sites where the pottery pieces were excavated were also collected to estimate the annual doses.

All procedures for the isolation of coarse quartz grain fractions have been done under the red light to avoid bleaching effects as low as possible. The samples were gently crushed in an agate mortar. Fine soil or clay constituents were washed out with water to allow relatively heavy and coarse grain parts to be collected. All grain fractions were treated with HCl solution. The etching procedure with concentrated HF for 6 hours followed to remove surface layer; then the surfaces were washed with water. After drying, heavy liquid separation (2.64-2.66 g/cm^3) with sodium polytungstate solution was carried out to purify the quartz fraction. Finally, quartz grains were sieved into 125-250 μm-sized particles.

2-2 Thermoluminescence color imaging and on-line TL-spectrometry

The characteristics of TL-coloration from quartz extracts were examined with a qualitative thermoluminescence color image (TLCI) technique and subsequently with an on-line TL-spectrometry (Hashimoto et al., 1997a).

Each TLCI was taken in the temperature range of 80 to 450^{o}C. Because further quantitative information of detection wavelengths was needed, the on-line TL-spectrometry was carried out for the grain samples using a highly sensitive spectrometric system that included an image-intensifier photo-diode array (IPDA) detector. Based on both TLCI and TL-spectrometric results, the combination of optical filters and photomultiplier tube could be appropriately selected.

In the practical RTL-measurements, a photomultiplier tube (PMT, Hamamatsu, R-649S) with multi-alkali (Na-K-Sb-Cs) photon detection part was installed together with a filter combination of a red-glass filter (Toshiba, R-60) and an infrared-cut filter (Eagle) to reduce blackbody radiation starting from longer wavelengths. The BTL-measurements were carried out using a PMT (Hamamatsu, R-585S) with bialkali-photon sensitive surface and a blue-glass filter (Toshiba, B-390). The optical transmission properties of these filter combinations are indicated for BTL and RTL measurements in Figure 1.

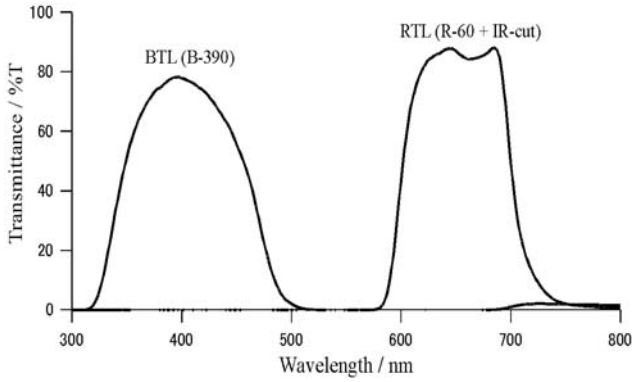

Figure 1.
Percentage transmittance as a function of wavelength for detection of RTL and BTL using optical filter combinations.

2-3 Luminescence measurements

All of the luminescence measurements were carried out using a new automated TL/OSL-reader system, which has been developed for the SAR-method (Hashimoto et al., 2002a, Fattahi, M. and Stokes, S., 2000). This system was especially focused on the RTL-measurements from minerals, which have been recently expected to provide reliable luminescence dating from both quartz and feldspar grains (Fattahi and Stokes, 2003). In the SAR-method, every luminescence measurement with high sensitivity is required to fulfill the same conditions as well as in the case of the artificial irradiation on mineral samples. The measuring requirement was realized by using a light guide made of a core rod-type glass pipe (68 mm length, 11 mm diameter, manufactured by Nissei Denki Co. Ltd.), inserted between a sample vessel for luminescence and a PMT-surface. The use of a glass light guide also helped the elimination of thermal noise from the heater due to non-thermal conductivity. The artificial irradiations with the desirable doses were obtained using a small X-ray irradiator (Varian, VF-50J tube with W-target, 50kV, 1mA, 50W at maximum operation) instead of a commonly available radioactive-source. The advantages of this X-ray irradiator include the availability of variable dose settings by adjusting both applied voltages and currents of the tube, simple radiation protection without heavy shielding material, and uniformity of irradiated areas ascertained also by Andersen et al. (2003). Additionally, the use of a cooling fan for heater assembly allowed rapid

recycling TL-measurements (Hashimoto et al., 2002a, b).

To minimize the influence of black-body radiation at higher temperature beyond 300°C, we made the heater area facing the PMT as small as possible. The heater was constructed by assembling four pieces of ceramic heater (heating power of 32Wx4) into one stack, which is readily controllable by a commercially available thermo-control unit (Okura, EC5800S). The background counts accompanied with rising temperature are shown in Fig. 2 in both cases of RTL and BTL-measurements. The present RTL-reader reveals an excellent low noise value (about 20 cps at 300°C), compared with a reference background of about 75 cps at 300°C (Fattahi and Stokes, 2000). This means that the present RTL-measuring system is applicable to the lower dose-samples, which leads to the possibility of recent sample dating and/or the necessity of small amounts of quartz grains for precious samples.

On the basis of preliminary experiments, the preheating condition after artificial irradiation was applied for 10 sec at 200°C. The weight of the measured sample was always fixed to 5 mg. Additionally, the sensitivity changes associated with repeated measurement (heating)/irradiation cycles were confirmed to provide only negligibly small contributions for both RTL- and BTL-measurements (Yawata & Hashimoto, 2004). Therefore, the SAR-method was employed here without any correction of sensitivity changes.

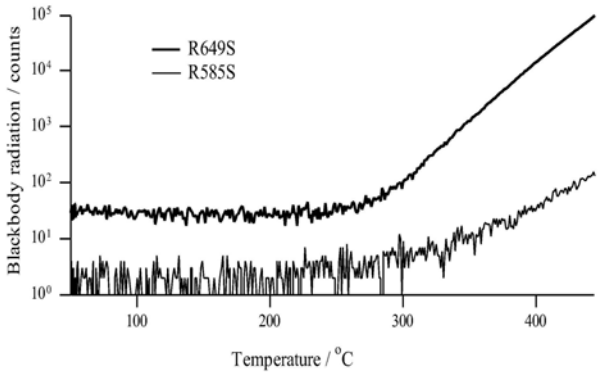

Figure 2.
Dark counting rate of a blank silver pan on new automated luminescence measuring system. The photomultiplier tube (PMT, Hamamatsu, R-649S) for RTL was cooled at -20°C, while the PMT for BTL (Hamamatsu, R-585S) was employed at room temperature. Filter combinations are described in Fig. 1.

2-4 Estimation of annual doses

Whenever the annual dose is evaluated from measurements of naturally occurring radioactivity for dried-soil material, the correction of water content in the as-received soil was required (Aitken, 1985). To estimate water contents, we dried the original soil samples on a hotplate. The heating condition was for 48h at 100°C. The dried soil and crushed pottery samples were packed into a cylindrical plastic container (U-8). The samples were subjected to the γ-ray spectrometry using a germanium coaxial p-type detector connected with a multi-channel analyzer (EGPC 120-210-R, EURISYS Measures). By assuming a homogeneous distribution, one can calculate natural annual doses from the radionuclide concentrations in the radioactive equilibrium within uranium and thorium decay chains (Aitken, 1985). The potassium, uranium, and thorium contents were determined by the photo-peaks at 1460 keV of ^{40}K and at 609 keV of ^{214}Bi for the U-series, and by the peak of 583 keV of ^{208}Tl for the Th-series, respectively.

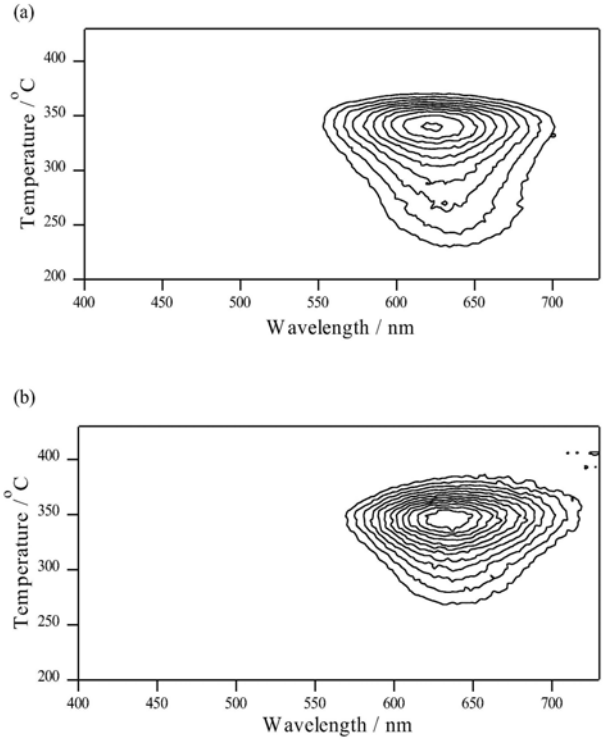

Figure 3.
Contour maps of artificially induced TL from quartz extracts from pottery pieces. The quartz extracts of about 10mg were irradiated to X-ray doses of 2.7kGy: (a) No. 5 pottery piece from Achiyadaira, (b) No. 8 pottery piece from Miyasori.

3 Results and discussion

3-1 TL-spectrometric results

Two typical contour maps are illustrated in Figs. 3(a) and 3(b). A typical single-RTL peak in the

red-spectrometric region, consisting of 620nm in wavelength and around 330°C, could be recognized in both the contour maps. All other quartz extracts from the present pottery pieces showed similar RTL-properties, in which an intense peak appears around 330-360°C in the red wavelength region of 600-650nm. These RTL-properties of quartz extracts were excellently concordant with the TL color images photographed by a color-sensitive film, although a few quartz extracts showed blue grain components, probably due to feldspar contamination. The present result has also confirmed that quartz extracts from other burnt relics or pottery pieces have given RTL-properties without almost any exception (Hashimoto et al., 2001). Additionally, this result could support the explanation that quartz slices fired beyond 900°C can change from BTL into RTL, which is consistent with the RTL-nature of quartz grains from the volcanic ash layers (Hashimoto et al., 1996, 1997b). In these pottery pieces, although most RTL might be attributable to the effects of archaeological firing, there remains still now some possibility of contamination of the as-received RTL quartz grains, which were provided from a volcanically originating layer into clay minerals as raw material of the pottery.

In addition to these red-regions of 600-700nm, the BTL (ranging of 350-500nm), which has been used appropriately for the TL-dating of quartz extracts, was also employed for the purpose of comparison with the present pottery dating.

3-2 Luminescence measurements and dating results

The changes of both RTL and BTL-glowcurves by applying the SAR-method are shown in Figs. 4(a) and 4(b), for quartz extracts from the pottery piece of Achiyadaira. In the RTL-glowcurves, there exists two intense peaks around 230°C and 350°C. The former was induced by artificial X-ray irradiation, because natural TL (NTL)-glowcurve does not present any peak in this region. Alternatively, the natural RTL-glowcurve offered a broad peak in the high temperature region beyond 300°C. The integration temperature range was determined from 290°C to 360°C by using plateau tests, consisting of ratios of ATL (artificial TL)- to NTL-glowcurve as a function of heating temperature.

On the other hand, the BTL-glowcurves consist of broad spectra over 200 to 400°C. Such glowcurves are often observed in the case of thermally annealed feldspar grains when a preheating procedure was applied with the similar condition of 200°C for 10 sec. We assumed that some proportion of feldspar constituent was contaminated in the quartz extracts. However, the BTL-integration was done in the high temperature regions of 340-380°C. A similar difference between RTL- and BTL-glowcurves has been reported by the RTL-dating of quartz from Quaternary volcanoes by Montret et al. (1992). These authors also suggested that some contamination of feldspar components could be seen in BTL-glowcurves.

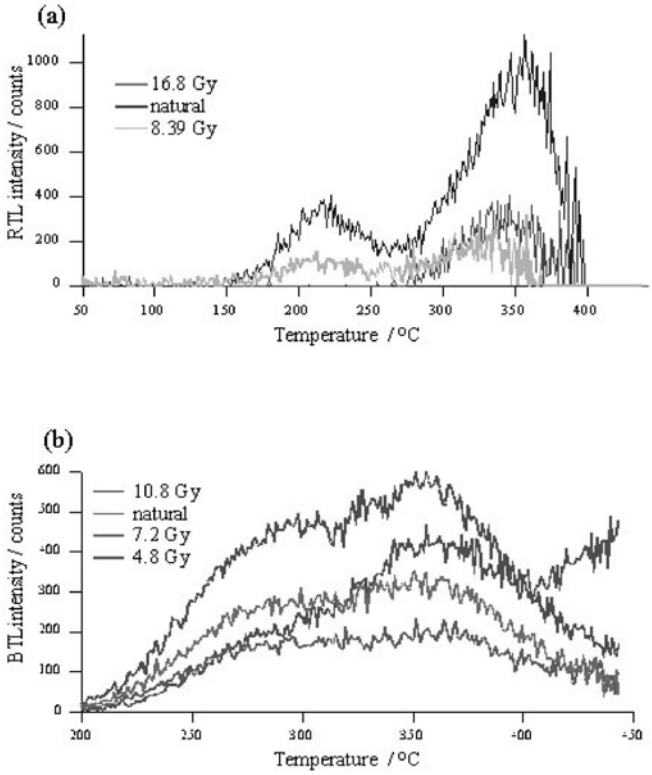

Figure 4.
Changes of glowcurves of RTL (a) and BTL (b) associated with artificial irradiation doses. Quartz extracts are obtained from No. 5 pottery piece.

The RTL- or BTL-values integrated over plateau regions as a function of regenerative doses brought on the corresponding response curves as shown in Figs. 5(a) and 5(b). It was noticed that every response curve of RTL from SAR-method gave different gradients from aliquot by aliquot, not only between different pottery pieces but also within the same piece. This means that the RTL-sensitivity properties reflect differently in each quartz grain as well as in each aliquot. In dose-response curves, the curves often give supralinear results over regenerative doses of 10-15Gy in many cases, so that the growth curves were fitted using a polynomial curve.

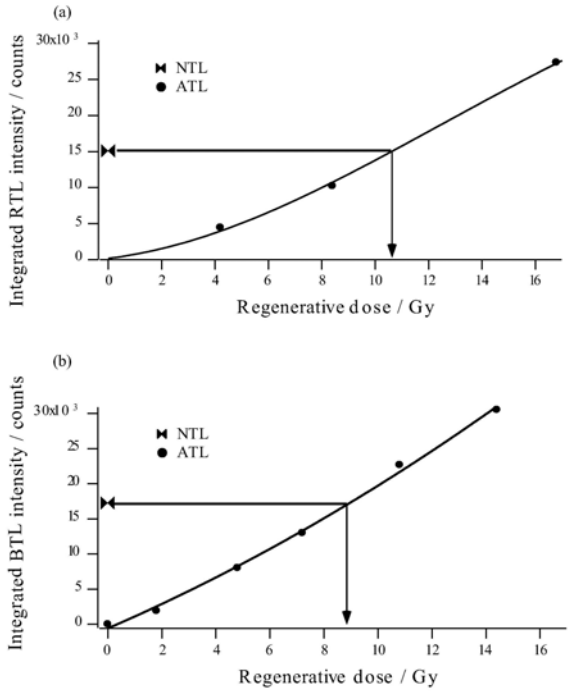

Figure 5.
Luminescence response curves as a function of regenerative doses. RTL (a) and BTL (b) are measured for a quartz aliquot from No. 5 pottery.

All results from RTL and BTL dating are summarized together with annual doses in Table 1. The experimental errors of equivalent doses are derived from two to four aliquot analyses. From the viewpoint of the equivalent doses, all of the RTL-values are found above 11.6Gy and up to 26.0Gy. On the other hand, the BTL-equivalent doses estimated usually give lower values than the RTL-ones. In four samples, no-BTL was detected even with the highly sensitive luminescence measuring system in our laboratory. It should be emphasized here that the quartz fractions from burnt samples such as pottery pieces tend to give the RTL-property, probably owing to the thermally heating process used during the manufacture of such material. Therefore, the RTL measurements are recommendable to evaluate accumulated dose.

The annual doses were evaluated from both crushed pottery pieces and surrounding soil. The former was used for β-ray contributions, while the latter was employed for γ-ray contributions by correcting water content. All annual doses are used to calculate mean value and standard deviations as indicated by two asterisks. There appears that two samples, including B-8 and B-10, differ greatly from the other pottery pieces. Since the radioactivity contents in the pottery are apparently dependent on the clay materials of pottery, these two pieces of pottery might be tentatively considered to have been manufactured in a different place from where the other pottery pieces were made.

The annual doses were utilized to calculate the TL-ages. The results are presented in the last three columns, together with ages predicted from the mode of pottery surface. Very good agreement exists between RTL-ages and the ones predicted within experimental errors. In advanced analysis, the authors are intending to improve RTL-measuring condition aiming towards the reduction of experimental errors, using the application of a single grain method (Yawata and Hashimoto., 2004). There exists a certain trend of giving shorter ages from BTL, as expected from the results of equivalent doses, in which some accumulated doses of BTL could not be detected. This underestimation of BTL-doses could arise from several factors, including the relatively unstable nature of BTL-source in comparison with the stable nature RTL (Hashimoto et al., 1993), tendency of BTL to bleach easily during sample storage, the presence of concomitant feldspar grains in the purified quartz fraction and so on. In the extreme case, the absence of BTL might introduce no-BTL emission in some burnt quartz. In fact, the BTL in quartz fractions from some volcanic origin has offered two or three orders lower than the RTL (Hashimoto et al., 1987).

The dominant presence of RTL-quartz has been recognized not only in materials of volcanic origin, but also in archaeologically burnt pottery. Consequently, the RTL from quartz grains has been considered a potentially useful dosimeter for the dating of thermal resetting events, such as archaeological burning of pottery, porcelain and stone as well as volcanic eruptions (Montret et al., 1992, Hashimoto and Fujita, 1999).

4. Conclusions

Most quartz grains extracted from burnt pottery pieces have shown strong RTL properties. Thus, the luminescence measurements involving RTL and BTL are applied to the estimation of the naturally accumulated doses for the quartz extracts from archaeologically burnt pottery pieces by applying the SAR-method.

The ages evaluated from RTL have revealed values in excellent agreement with the expected ages, whereas BTL gave relatively lower values or no-information about ages. Conclusively, the RTL-dating will be recommended for quartz extracts from archaeologically burnt pottery.

Some pure quartz grains without so much impurity, that originated from plutonic rocks, could be applied generally to the existing BTL-dating. In fact, Madagascar quartz slices of hydro-thermal

Pottery pieces	mode of Jomon pottery or Jomon stage	RTL equivalent dose (Gy)	BTL equivalent dose (Gy)	Annual dose (mGy/y)	RTL age (years B.P.*)	BTL age (years B.P.)	Predicted age (years B.P.)
Achiyadaira							
A-5	Minamisanjuinaba	13.1 +/- 4.0	6.3 +/- 1.4	3.47 +/- 0.11	3800 +/- 1150	1800 +/- 410	4000
A-8	Shinbo	17.3	n.d.	3.27 +/- 0.11	5300 +/- 180	n.d.	5000
A-14	KasoriB3	14.7 +/- 2.1	13.3	3.17 +/- 0.11	4600 +/- 670	4200 +/- 150	3500
B-8	later period of early stage	11.6 +/- 3.3	4.4 +/- 2.2	2.17 +/- 0.10	5300 +/- 1520	2000 +/- 1000	6000
B-10	middle period of early stage	14.8 +/- 3.5	9.3 +/- 0.8	2.18 +/- 0.09	6800 +/- 1640	4300 +/- 410	6000
B-12	early period of early stage	26.0 +/- 2.2	n.d.	3.69 +/- 0.12	7000 +/- 630	n.d.	6000
Shimozori							
A-18	later period of late stage	15.0 +/- 2.4	1.47	3.44 +/- 0.11	4400 +/- 710	430 +/- 10	5000
Miyasori							
A-23	Hanadumikasou	22.7 +/- 2.9	n.d.	3.01 +/- 0.11	7500 +/- 1000	n.d.	6000
Motoyashiki							
B-18	later period of late stage	12.2 +/- 1.0	n.d.	3.17 +/- 0.13	3800 +/- 360	n.d.	3500
				3.06 +/- 0.51 **		n.d. : Not determined	

* : B.P. : before present (2000)
** : mean and standard deviation

Table 1.
Comparison of equivalent doses and luminescence ages for pottery pieces using RTL- and BTL-measurements of quartz extracts.

origin showed that some parts retain BTL-properties while some parts with high Al-impurity changed from BTL- into RTL-properties after annealing at a high temperature beyond 900°C (Hashimoto et al., 1996, 1997b). In all cases, the accurate TL-dating of archaeologically burnt materials should be carried out after judging whether TL-properties of quartz extracts are RTL or BTL.

Acknowledgements
The authors wish to express their gratitude to Mr. Yasuo Takahashi, a chief director of the Asahi-machi Culture Research Center, Niigata, Japan, for providing archaeological pottery pieces and for valuable information and discussions. We would like to express our appreciation to Professor F. S. Howell of The Sophia University, Tokyo, for kind corrections of the manuscript.

References

Aitken, M. J., 1985. Thermoluminescence dating. Academic Press, London.

Andersen C. E., Boetter-Jensen L., and Murray A. S., 2003. A mini X-ray generator as an alternative to a $^{90}Sr/^{90}Y$ beta source in luminescence dating. *Radiat. Meas*., **37**, 557-561.

Fattahi, M. and Stokes, S., 2000. Red thermoluminescence (RTL) in volcanic quartz: development of a high sensitivity detection system and preliminary findings. *Ancient TL*, **18**, 35-44.

Fattahi, M. and Stokes, S., 2003. Dating volcanic and related sediments by luminescence methods: a Review. *Earth-Sci. Rev.*, **1280**, 1-36.

Hashimoto, T., Koyanagi, A., Yokosaka, K., and Sotobayashi , Y., 1986. Thermoluminescence color images from quartz of beach sands, *Geochem. J*., **20**, 111-118.

Hashimoto, T., Yokosaka, K., and Habuki, H., 1987. Emission properties of thermoluminescence from natural quartz-blue and red TL response to absorbed dose. *Nucl. Tracks Radiat. Meas.*, **13**, 57- 66.

Hashimoto, T., Sakai, T., Shirai, N., Sakaue, S., and Kojima, M., 1991. Thermoluminescent spectrum changes of natural quartz dependent on annealing treatment and aluminum-contents. *Anal. Sci*., **7**, 687-690.

Hashimoto, T., Kojima, M., Shirai, N., and Ichino, M., 1993. Activation energies from blue and red-thermoluminescence (TL) of quartz grains and mean lives of trapped electrons related to natural red-TL. *Nucl. Tracks Radiat. Meas*., **21**, 217-223.

Hashimoto, T., Sakaue, S., Aoki, H., and Ichino, M., 1994. Dependence of TL-property changes of natural quartzes on aluminium contents accompanied by thermal annealing. *Radiat. Meas*.. **23**, 293-299.

Hashimoto, T., Notoya, S., Ojima, T., and Hoteida, M., 1995. Optically stimulated luminescence (OSL) and some other luminescence images from granite samples exposed with radiations. *Radiat. Meas*.. **24**, 227-237.

Hashimoto, T., Notoya, S., Arimura, T., and Konishi, M., 1996. Changes in luminescence colour images from quartz slices with thermal annealing treatments. *Radiat. Meas*.. **26**, 233-242.

Hashimoto, T., Sugai, N., Sakaue, H., Yasuda, K., and Shirai, N., 1997a. Thermoluminescence (TL) spectra from quartz grains using on-line TL-spectrometric system. *Geochem. J*., **31**, 189-201.

Hashimoto, T., Katayama, H., Sakaue, H., Hase, H., Arimura, T., and Ojima, T., 1997b. Dependence of some radiation-induced phenomena from natural quartz on hydroxyl-impurity contents. *Radiat. Meas.*, **27**, 243-250.

Hashimoto, T., and Fujita, H., 1999. Dating using red-thermoluminescence (In Japanese). *Chikyu (The Earth)*, **26**, 109-114.

Hashimoto, T., Komatsu, Y., Hong, D. G., and Uezu Y., 2001. Determination of radioactivenuclides in small pieces of archaeological sample and its application to TL-dating. *Radiat. Meas*., **33**, 95-101.

Hashimoto, T., Nakagawa, T., Hong, D. G., and Takano, M., 2002a. An automated system for both red / blue thermoluminescence and optically stimulated luminescence measurement. *J. Nucl. Sci. Technol*., **39**, 108-109.

Hashimoto, T., Nakagawa, T., Usuda, H., and Yawataa, T., 2002b. Development of an automated system equipped with a small X-ray irradiator for red/blue thermoluminescence and optically stimulated luminescence measurement from natural minerals (in Japanese). *BUNSEKI KAGAKU*, **51**, 625-632.

Hashimoto, T., Yamaguchi, T., Fujita, H., and Yanagawa, Y., 2003. Comparison of infrared spectrometric characteristics of Al-OH impurities and thermoluminescence patterns in natural quartz slices at temperature below 0^{o}C. *Radiat. Meas*., **37**, 479-485.

Miallier, D., Faïn, J., Sanzelle, S., Pilleyre, S., Montret, M., Soumana, S., and Falguères, C., 1994. Attempts at dating pumice deposits around 580 ka by use of red TL and ESR of xenolithic quartz inclusion. *Radiat. Meas*., **23**, 399-404.

Montret, M., Miallier, D., Sanzelle, S., Faïn, J., Pilleyre, TH., and Soumana, S., 1992. Tl dating in the Holocene using red TL from quartz. *Ancient TL*, **10**, 33-36.

Wintle, A. G., Murray, A. S., 2000. Quartz OSL: Effects of thermal treatment and their relevance to laboratory dating procedures. *Radiat. Meas*.. **32**, 387-400.

Yawata, T., and Hashimoto, T., 2004. Identification of the volcanic quartz origins from dune sand using a single grain RTL-measurement. *Quart. Sci. Rev*., **23**, 1183-1186.

Reviewer

D. Miallier

A method for quickly estimating the equivalent dose in optical dating of K-feldspar

A.M.J. Hamel and D.J. Huntley

Department of Physics, Simon Fraser University, Burnaby, BC V5A 1S6, Canada

(Received 18 March 2004; in final form 25 May 2004)

Introduction

In optical dating, before one can actually determine an age, the sample must go through several processes of washing, drying and grain selection that take considerable time. It sometimes happens that the sample collected has an optical age very much larger than expected. This can happen for example if sampling had yielded material from below a sand dune rather than from the dune itself as intended; it would also occur if the sample desired was obtained, but was not bleached before burial. The purpose of the experiment described below was to determine whether or not a useful preliminary estimation of a sample's equivalent dose and age could be obtained quickly. Raw sand was used for the aliquots, which were measured, given a radiation dose, heated, measured once more, and the equivalent dose estimated. It is found that this method can save grain preparation time and effort if a sample is not what it is thought to be, and may replace the usual pilot experiment to determine the appropriate radiation doses to give prepared grains for optical dating.

Experimental procedure

Twenty samples were chosen from our collection to test the method on a wide range of D_{eq}'s. For each, an equivalent dose and optical age has been obtained using a standard multiple aliquot method on separated K-feldspar grains in a particular size range. For each sample, raw sediment was taken from the original sample to fill three planchets. This means no removal of carbonates, no grain size selection, no magnetic separation, no density separation, no drying. To stick the grains to the planchets, we put a few drops of a thermoplastic polymer (Crystalbond[1]) dissolved in acetone in each planchet, put the raw sediment in and covered the grains with more of this "glue". Then all planchets were heated at 50 °C for an hour so that the acetone would evaporate and the polymer would harden. Except where indicated otherwise, all samples are sand.

[1] Crystalbond 509: Aremco Products Inc., P.O. Box 517, 707-B Executive Blvd., Valley Cottage, N.Y. 10989, U.S.A.

1.4 eV (infrared) light from light-emitting diodes (LED's) were used for excitation, and the emission was measured using a Thorn-EMI 9635Q photomultiplier tube and photon-counting electronics. Schott BG-39 and Kopp 5-57 filters were placed in front of the tube to absorb infrared light and to pass the violet emission that is characteristic of K-feldspars.

A first measurement was done on the natural aliquots; the excitation lasted five seconds during which the emission decreased by ~7 %. Then radiation doses of ~60 Gy were given, this dose being chosen to be about twice the largest expected D_{eq}. All aliquots were then heated at 120°C for 16 hours and measured promptly after cooling, using the same conditions as for the first measurement.

Results

For each aliquot, a linear dose response was assumed and the equivalent dose calculated as:

$$D_{eq} = lab.\,radiation\ dose \times \frac{natural\ count}{dose\ count - natural\ count}$$

where the natural count is the sum of the photon counts (minus background counts) from the first measurement, and the dose count is the sum of the photon counts (minus background counts) from the second measurement.

Comparisons of the equivalent doses estimated this way with those obtained earlier using a standard multiple aliquot method are given in Fig.1 and Table 1. We also wanted to see how good an estimate of the age can be obtained by this method, and to this end have calculated an estimated age using an effective dose rate of 2 Gy/ka. Comparison of these ages with the ages obtained previously with the standard method is shown in Table 1.

Discussion

Fig.1 gives evidence of the validity of the raw sand method in estimating equivalent doses. For samples over ~300 years old the estimated values are within a factor of two of the known D_{eq}'s. Differences are expected to be caused by a variety of effects,

Sample	Equivalent dose (Gy)		Age (ka)	
	multiple aliquot	estimated	multiple aliquot	estimated
SAW03-03	0.00 ± 0.11	0.48	0.000 ± 0.036	0.2
BUCT5-1	0.01 ± 0.08	0.12	0.005 ± 0.030	0.06
SAW03-02	0.06 ± 0.15	0.23	0.021 ± 0.053	0.1
SNO2	0.08 ± 0.01	0.09	0.050 ± 0.007	0.04
SAW01-12	0.30 ± 0.04	0.22	0.14 ± 0.02	0.11
SAW03-04	0.37 ± 0.10	1.19	0.161 ± 0.047	0.6
IC5-02	0.62 ± 0.05	1.37	0.260 ± 0.026	0.68
SAW03-01	0.87 ± 0.10	1.22	0.329 ± 0.046	0.6
CBTS2	2.09 ± 0.13	1.7	1.285 ± 0.095	0.84
BUCT1-1	2.32 ± 0.08	2.4	0.765 ± 0.045	1.2
SNH3	3.15 ± 0.04	4.5	2.08 ± 0.09	2.3
SAW01-06	3.24 ± 0.08	2.4	1.66 ± 0.08	1.2
SN27	7.13 ± 0.14	8.4	5.47 ± 0.24	4.2
IC4-01	10.8 ± 0.8	13.5	4.54 ± 0.42	6.8
SW6-01	10.9 ± 0.3	12.9	4.19 ± 0.20	6.5
LCP5 (peat)	18.8 ± 0.5	18.7	31.2 ± 2.6	37
SAW01-27	25.5 ± 0.7	27.8	15.05 ± 0.97	14
CCL2 (loess)	28.9 ± 2.1	23.4	11 ± 1	12
DY24	36.3 ± 1.2	74	14.7 ± 1.3	37
SAW01-16	in saturation	in saturation		

Table 1.
Comparison of the estimates of equivalent doses and ages using the method described here, with those obtained using a conventional multiple aliquot method. Estimated equivalent doses were determined for three aliquots for each sample and the average taken. Estimated ages were deduced from them assuming the effective equivalent dose rate to be 2 Gy/ka, except for LCP5, a peat, for which 0.5 Gy/ka was assumed.

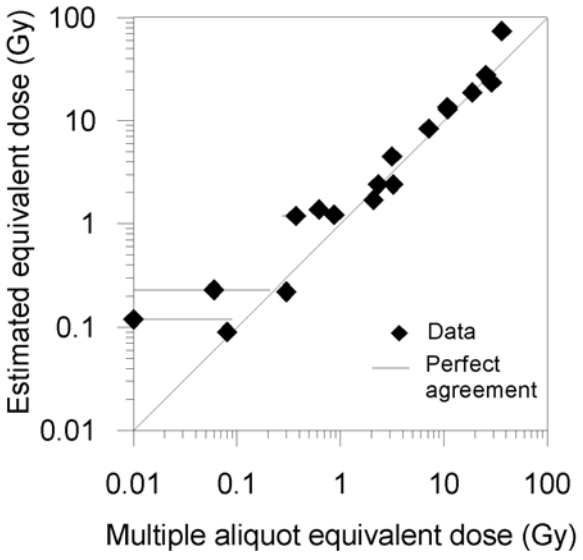

Figure1.
Comparison of estimated and previously determined equivalent doses.

including the variety of grain sizes, the possible presence of minerals other than K-feldspar responding to 1.4 eV excitation, the draining during the first measurement, and some shallow traps being emptied by the heating before the second measurement but not before the first.

In cases where the estimated equivalent dose is similar to that obtained using the standard method, the age obtained using the assumed effective dose rate is generally also reasonable. Hence, if the estimated age is very much higher than expected, it can indicate a lack of exposure to sunlight prior to burial or that the sediment being dated does not correspond to the event for which the dating is intended. The latter could also explain an estimated age much lower than expected. Both situations show the advantages of using this method before starting to prepare a sample for serious dating. In addition, saturation of the traps is very well detected with the method (see SAW01-16); here the dose count is similar to the natural count. Knowing all this, one will not waste time and effort preparing the sediment to find out only later that it cannot be dated.

If one used a shorter, higher-temperature heating and larger dose rate than we used, one could get results within a single day.

The method may be useful for some samples older than those reported on here, but the non-linear dose response will introduce an increasingly large error. It may be possible to modify the equation for D_{eq} to allow for this but this is speculation and requires further experimentation.

Li and Wintle (1994) and Lian and Huntley (1999) earlier sought to extract chronological information from unseparated sediments and appear to have been successful with their different objectives. The experiment of Li and Wintle was similar to ours, but they used a UV exposure instead of the γ-radiation dose, thus they did not obtain D_{eq} estimates. They then measured the response to a dose and suggested a method of obtaining D_{eq} estimates that deals with the non-linear response at high doses.

Acknowledgements

The Natural Sciences and Engineering Research Council of Canada is thanked for financial support. We thank the various scientists who provided samples or assisted with their collection, and G.A.T.Duller for suggestions for improving the ms.

References

Li, S.-H. and Wintle, A.G. 1994. Use of infra-red stimulated signals from pellets of compressed loess from Rocourt, Belgium. Quaternary Science Reviews 13, 519-532.

Lian, O.B. and Huntley, D.J. 1999. Optical dating studies of post-glacial aeolian deposits from the south-central interior of British Columbia, Canada. Quaternary Science Reviews 18, 1453-1466.

Rewiever

Geoff Duller

Obituary

Georges VALLADAS
(January 1920 – February 2004)

Georges VALLADAS was born into a very modest family, a situation which limited his educational opportunities. Nevertheless, at the age of 17 he entered the prestigious laboratory of Paul Langevin in College de France as a technician. While there he was able to pursue his studies and obtain an engineering degree.

At the end of the second world war, he was one of the first engineers recruited by the new CEA (French Atomic Energy Commission) in 1946. The Commission was responsible for the construction of the first French Atomic Reactor, Zoe, and later for the development of nuclear research, both fundamental and applied. Georges' first task was to design and construct boron fluoride ionization chambers to measure the neutron flux near the core of Zoe. These chambers monitored the start of the reactor on December 15, 1948.

Soon after, Georges became interested in fundamental physics and moved into the Nuclear Physics Department where he developed an impulsion ionization chamber designed to study the alpha fine structure of some heavy nuclei. In 1954, he defended his Ph.D. dissertation on the spectrometry of alpha rays and its applications. He briefly left France in 1956 to work in Liverpool, at the synchro-cyclotron Laboratory, and, subsequently stayed a number of times at the CERN Laboratory in Geneva to develop detectors in the very high energy range.

In 1972, he joined the Centre des Faibles Radioactivités in Gif/Yvette, near Paris. A that time, as there were no commercial TL readers, Georges designed and built his own TL readers of high performance, accuracy and sensitivity for multiple grain studies. He also developed a special equipment dedicated to single grain measurements. Some of his apparatus is still being used in the Gif Laboratory. Busy as he was with his own research Georges nevertheless found time to offer advice, plans, and even complete equipment for others. Quite a few TL laboratories in France (Univ. Paris VI, Clermont-Ferrand, Fontenay-aux-Roses, Strasbourg...), whether in the field of Archeological or Geological Dating, or in the field of Radioprotection benefited from his help.

Not content with building the equipment Georges pursued miscellaneous dosimetric studies and applications of TL. He became interested in the dating of meteorites, lunar samples and volcanic activity. He and G. Guérin got around the problem of anomalous fading in feldspars, by measuring the high temperature (>600 °C) TL emission of plagioclases. He also worked on quartz samples which enabled him to date the Laschamp lava flow (Chaîne-des-Puys), contemporaneous with the terrestrial magnetic field excursion of the same name.

During the two decades preceding his retirement, Georges became interested in the TL dating of Palaeolithic and developed a protocol which allowed for burnt flints from prehistoric hearths to provide dates for sites beyond the reach of radiocarbon techniques. Burnt flints from several key-sites have yielded ages which have radically modified the accepted chronology for the presence of Neanderthal and Moderns Humans in the Near East and Europe.

Georges Valladas maintained full scientific activity well beyond retirement age, until health problems forced him to slow down in 1995. His long professional life has been the life of a very talented physicist, a builder of high quality equipment, a great experimentalist. In recognition of his work he was awarded the Silver Medal of CNRS. He was held in great esteem internationally, particularly in the small world of Thermoluminescence, where he was ranked among the pioneers of TL Dating.

As a scientist, Georges was a hardworking person noted for his helpfulness, generosity, modesty, and unselfish devotion to Science.

Raphaël Visocekas
Jean Faïn
Didier Miallier
Gilles Guérin
Norbert Mercier
Serge Sanzelle

Thesis Abstracts

Thesis title: An investigation into the physics of the infrared excited luminescence of irradiated feldspars

Author: Michael Anthony Short
Grade: Ph.D.
Date: January 2003
Supervisor: D. Huntley
University: Simon Fraser

Infrared excitation of irradiated feldspars produces a luminescence glow in one or more broad emission bands. The processes are poorly understood, but they are suspected to occur in lattice defects, although their general identity is unknown. This thesis is about trying to understand more about the physics of these processes. I found the emission intensity increased as the temperature was increased above 20 C for emission bands with peak intensities at wavelengths around 330, 400 and 570 nm, but the rate of increase dropped off for some samples as the temperature was increased over 80 C. These results were interpreted as being due to the excitation of different vibrational modes of the feldspar structure. The rate of decay in the emission intensity of one sample was independent of temperature. The latter was clear evidence against a model where charge is excited from a trap by a combination of both optical and thermal excitation. The emission intensities of some emission bands were dependent on the polarization of the infrared exciting light, and the emission itself was polarized in some cases. These results were explained by dipolar transitions occurring within unknown defect centres located at either the T1, M or OD lattice sites. This explanation was supported by studies on transitions within Fe+3 ions occupying known lattice sites. I also found that there was a small photoconductivity with green light excitation, but no measurable effect with infrared excitation. However I could not rule out the possibility that charge was excited to delocalised bands in both cases. A model is proposed to explain these results with one basic type of electron trap which is excited by the infrared light. The excited electron can either tunnel through to a recombination centre or it can be thermally excited to the conduction band or to a state just below the conduction band. Anion defects are shown to be possible centres for the traps. Changes in the fraction of electrons that tunnel to the recombination centres, and electron spin interactions are proposed as additional mechanisms that may also have some effect on the changes in emission intensity with temperature.

(Due to an editing mistake a wrong text was associated to the thesis abstract by M.A. Short in Ancient TL 21No.1).

Thesis title: Contribution of luminescence dating to the chronology of Middle Stone Age techno-complexes associated with the first South African modern humans.

Author: Chantal Tribolo
Grade: Ph.D.
Date: October 2003
Supervisors: N. Mercier , J. -J. Hublin
University: Bordeaux I

Key words: Middle Stone Age, Howieson's Poort, Still Bay, modern Humans, South Africa, TL/OSL, burnt quartzites and silcretes

Thesis available on line (pdf file)
http://147.210.235.3/proprietes.html?numero_ordre=2725

The chronology of the evolution of anatomically modern human behaviour is a highly controversial subject. One would like to know if some behaviours considered typical of the Late Stone Age (LSA) appeared during that period, or much earlier during the Middle Stone Age (MSA). Two techno-complexes of the South African MSA, the Howieson's Poort and the Still Bay, are particularly relevant to this question since some of the stone tools are typical of the MSA period whereas others have characteristics usually associated with the LSA "modern" behaviour, like standardisation and choice of exotic materials. Stratigraphic observations as well as prior dating work have shown that these two techno-complexes originated well within the MSA. However, more precise chronology was lacking. The aim of the work summarised here was to refine this chronology by applying luminescence dating methods to burnt stones selected from three South African MSA sites: Blombos Cave, Diepkloof Rock Shelter and Klasies River. The stones were quartzites and silcretes both rich in quartz grains.

To determine the equivalent dose (Ed), the thermoluminescence (TL) as well as the optically stimulated luminescence (OSL) techniques were used, with respectively, a multiple aliquot additive and regenerative protocol and the single aliquot regenerative-dose protocol. It was observed that the

OSL signal was bleached if the stones were not protected from light as soon as discovered, even if they looked opaque to the eye. However, bleaching experiment indicated that the TL signal was still usable for the determination of the Ed and for some samples, linearly modulated OSL proved most suitable.

The external dose rate was measured by $CaSO_4$ dosimeters and the state of disequilibrium of the Uranium chain in the sediment samples determined by high resolution gamma spectrometry. In the case of Diepkloof Rock Shelter, the high spatial variation of the gamma dose rate precluded a precise calculation of the age. However, a preliminary interval was derived from the highest and lowest possible dose rates.

For the internal dose rate calculation, a model analogous to the one used for sediment dating was selected after an assumption of homogeneous distribution outside the quartz grains. The dose rate was calculated for each sample by combining the mean concentration of the radioisotopes, measured by the neutron activation technique, and the size distribution of the quartz grains in each stone, deduced from an image analysis of thin sections. For the Howieson's Poort layers at Diepkloof Rock Shelter a preliminary age-estimate of 55-65 ka was calculated. At Klasies River 13 age estimates averaging 56+-3 ka were obtained for the Howieson's Poort sequence, in good agreement with TL/OSL and ESR estimates for the same stratum. These new results, however, contradict certain hypotheses derived from palaeoenvironmental studies. At Blombos Cave, five lithic specimens yielded an average age of 74+-5 ka for the Still Bay level. This estimate is in good agreement with OSL and ESR results. It confirms that the Still Bay complex is older than the Howieson's Poort and sets back the beginnings of certain practices such as the use of symbols and work of bone to at least the isotopic stage 5.

Thesis title: Luminescence investigations and dating of anthropogenic palaeosols from South Mainland Shetland

Author: Christopher Ian Burbidge
Grade: PhD
Date: September 2003
Supervisors: Dr G.A.T. Duller, Prof R.A. Dodgshon; examiners: Prof I.K. Bailiff, Dr A.P. Rowlands
University: University of Wales Aberystwyth

This thesis aims to produce a chronostratigraphy of agricultural activity and sedimentary accumulation at two archaeological sites in the Shetland Islands, by directly dating the infield sediments associated with the sites. Optically stimulated luminescence (OSL) dating of a large number of samples, from often inhomogeneous sediments expected to have been subject to post-depositional mixing, is described. The samples were collected at high spatial resolution both vertically through sections, and horizontally within layers, to assess the consistency of results at different scales.

A novel approach to *in situ* environmental dose rate determination was pursued, using aluminium oxide dosimeters to measure the combined beta, gamma and cosmic radiation fields at the points of sampling. This yielded rapid and accurate measurements of environmental dose rate for the large numbers of samples taken from inhomogeneous dose rate environments.

Detailed investigation of the luminescence behaviour of quartz separates from a limited number of samples was used to optimise measurement conditions within the single aliquot regeneration (SAR) protocol. These optimised conditions were used in a simplified measurement protocol based on a standardised growth curve, which enabled the measurement of equivalent dose (D_e) distributions for small aliquots from large numbers of samples. A novel approach to direct assessment of error on the D_e was applied.

The observed D_e distributions were analysed using a model selection approach. Most distributions were found to be consistent with simpler representations than expected. However, the results from some samples indicated the presence of multiple populations in the data. Ages calculated from these results were used to assess different components in some of the archaeological deposits. However, their occurrence was not strongly associated with evidence for tilling of the soils or bioturbation.

Chronostratigraphies were established for both the infield deposits at Old Scatness Broch and the Sumburgh Hotel Gardens site using dates from 66 samples. The infield at Old Scatness contained soils, middens, and sands accumulated between the Bronze-Iron Age transition (~300 BC) and the 20th century. The Sumburgh Hotel Gardens site contained occupation deposits, sand and soils, mainly dating to the Early Bronze Age (~1500 BC). Quantitative estimates were made of the anthropogenic input to the soils at Old Scatness during the Iron Age.

Bibliography
(from 1st April 2003 to 31th March 2004) Compiled by Ann Wintle

---

Part 1: from 1st April 2003 to 30 September 2003

Basun, S., Imbusch, G. F., Jia, D. D. and Yen, W. M. (2003). The analysis of thermoluminescence glow curves. *Journal of Luminescence* **104**, 283-294.

Bateman, M. D., Thomas, D. S. G. and Singhvi, A. K. (2003). Extending the aridity record of the Southwest Kalahari: current problems and future perspectives. *Quaternary International* **111**, 37-49.

Berger, G. W. (2003). Luminescence chronology of late Pleistocene loess-paleosol and tephra sequences near Fairbanks, Alaska. *Quaternary Research* **60**, 70-83.

Bird, M. I., Turney, C. S. M., Fifield, L. K., Smith, M. A., Miller, G. H., Roberts, R. G. and Magee, J. W. (2003). Radiocarbon dating of organic- and carbonate-carbon in Genyornis and Dromaius eggshell using stepped combustion and stepped acidification. *Quaternary Science Reviews* **22**, 1805-1812.

Bogatikov, O. A., Gurbanov, A. G., Koschug, D. G., Gazeev, V. M. and Shabalin, R. V. (2002). The EPR of the rock-forming quartz from volcanic rocks of the Elbrus Volcano, Northern Caucasus, Russia. *Doklady Earth Sciences* **385**, 570-573.

Bowler, J. M., Johnston, H., Olley, J. M., Prescott, J. R., Roberts, R. G., Shawcross, W. and Spooner, N. A. (2003). New ages for human occupation and climatic change at Lake Mungo, Australia. *Nature* **421**, 837-840.

Cazenave, S., Chapoulie, R. and Villeneuve, G. (2003). Cathodoluminescence of synthetic and natural calcite: the effects of manganese and iron on orange emission. *Mineraology and Petrology* **78**, 243-253.

Chamyal, L. S., Maurya, D. M. and Raj, R. (2003). Fluvial systems of the drylands of western India: a synthesis of Late Quaternary environmental and tectonic changes. *Quaternary International* **104**, 69-86.

Clarke, M. L., Vogel, J. C., Botha, G. A. and Wintle, A. G. (2003). Late Quaternary hillslope evolution recorded in eastern South African colluvial badlands. *Palaeogeography, Palaeoclimatology, Palaeoecology* **197**, 199-212.

Correcher, V., Molina, D. and Garcia-Guinea, J. (2003). Effect of radiation on thermoluminescent properties of lava (in Spanish). *Revista Mexicana de Fisica* **49**, 235-241.

Curnoe, D., Grün, R. and Thackeray, J. F. (2002). Electron spin resonance dating of tooth enamel from Kromdraai B, South Africa. *South African Journal of Science* **98**, 540-540.

De Corte, F., Hossain, S. M., Jovanovic, S., Dlabac, A., De Wispelaere, A., Vandenberghe, D. and Van den Haute, P. (2003). Introduction of Marinelli effective solid angles for correcting the calibration of NaI(Tl) field gamma-ray spectrometry in TL/OSL dating. *Journal of Radioanalytical and Nuclear Chemistry* **257**, 551-555.

Duller, G. A. T. and Murray, A. S. (2000). Luminescence dating of sediments using individual mineral grains. *Geologos* **5**, 87-106.

Duttine, M., Villeneuve, G., Poupeau, G., Rossi, A. M. and Scorzelli, R. B. (2003). Electron spin resonance of Fe3+ ion in obsidians from Mediterranean islands: application to provenance studies. *Journal of Non-crystalline Solids* **323**, 193-199.

Dykeman, D. D., Towner, R. H. and Feathers, J. K. (2002). Correspondence in tree-ring and thermoluminescence dating: a protohistoric Navajo pilot study. *American Antiquity* **67**, 145-164.

Erfurt, G., Krbetschek, M. R., Bortolot, V. J. and Preusser, F. (2003). A fully automated multi-spectral radioluminescence reading system for geochronometry and dosimetry. *Nuclear Instruments and Methods in Physics Research B* **207**, 487-499.

Fattahi, M. and Stokes, S. (2003). Dating volcanic and related sediments by luminescence methods: a review. *Earth-Science Reviews* **62**, 229-264.

Feathers, J. K. (2003). Use of luminescence dating in archaeology. *Measurement Science and Technology* **14**, 1493-1509.

Ferko, T. E., Wang, M. S., Hillegonds, D. J., Lipschutz, M. E., Hutchison, R., Franke, L., Scherer, P., Schultz, L., Benoit, P. H., Sears, D. W. G., Singhvi, A. K. and Bhandari, N. (2002). The irradiation history of the Ghubara (L5) regolith breccia. *Meteoritics and Planetary Science* **27**, 311-327.

Finch, A. A., Hole, D. E. and Townsend, P. D. (2003). Orientation dependence of luminescence in plagioclase. *Physics and Chemistry of Minerals* **30**, 373-381.

Godfrey-Smith, D. I. and Casey, J. L. (2003). Direct thermoluminescence chronology for Early Iron Age smelting technology on the Gambaga Escarpment, Ghana. *Journal of Archaeological Science* **30**, 1037-1050.

Godfrey-Smith, D. I., Vaughan, K. B., Gopher, A. and Barkai, R. (2003). Direct luminescence chronology of the epipaleolithic Kebaran site of Nahal Hadera V, Israel. *Geoarchaeology* **18**, 461-475.

Hansen, E. C., Arbogast, A. F., Packman, S. C. and Hansen, B. (2003). Post-Nipissing origin of a backdune complex along the southeastern shore of Lake Michigan. *Physical Geography* **23**, 233-244.

Hashimoto, T., Nishiyama, E. and Yanagawa, Y. (2003). Radiation-induced luminescence and hydrogen radical formation associated with thermal annealing treatments on feldspars. *Journal of Radioanalytical and Nuclear Chemistry* **255**, 81-85.

Haustein, M., Roewer, G., Krbetschek, M. R. and Pernicka, E. (2003). Dating archaeometallurgicaol slags using thermoluminescence. *Archaeometry* **45**, 519-530.

Hesse, P. P., Humphreys, G. S., Selkirk, P. M., Adamson, D. A., Gore, D. A., Nobes, D. C., Price, D. M., Schwenninger, J.-L., Smith, B., Tulau, M. and Hemmings, F. (2003). Late Quaternary aeolian dunes on the presently humid Blue Mountains, Eastern Australia. *Quaternary International* **108**, 13-32.

Hong, D. G., Galloway, R. B., Kim, M. J. and Park, S. B. (2003). Optical dating of the hydroponic farm at Korea. *Journal of Radioanalytical and Nuclear Chemistry* **256**, 365-368.

Hormes, A., Preusser, F., Denton, G., Hajdas, I., Weiss, D., Stocker, T. F. and Schluchter, C. (2003). Radiocarbon and luminescence dating of overbank deposits in outwash sediments of the Last Glacial Maximum in North Westland, New Zealand. *New Zealand Journal of Geology and Geophysics* **46**, 95-106.

Hossain, S. M., De Corte, F., Vandenberghe, D. and Van den Haute, P. (2003). Annual radiation dose determination in the luminescence dating of Ossendrecht sand; specific problems and procedures. *Czechoslovak Journal of Physics* **53**, A257-A263.

Hossain, S. M., De Corte, F., Vandenberghe, D. and Van den Haute, P. (2003). The role of k(0)-NAA in the assessment of the annual radiation dose for use in TL/OSL dating of sediments. *Journal of Radioanalytical and Nuclear Chemistry* **257**, 639-642.

Jacobs, Z., Duller, G. A. T. and Wintle, A. G. (2003). Optical dating of dune sand from Blombos Cave, South Africa: II - single grain data. *Journal of Human Evolution* **44**, 613-625.

Jacobs, Z., Wintle, A. G. and Duller, G. A. T. (2003). Optical dating of dune sand from Blombos cave, South Africa: I - multiple grain data. *Journal of Human Evolution* **44**, 599-612.

Jain, M. and Tandon, S. K. (2003). Quaternary alluvial stratigraphy and palaeoclimatic reconstruction at the Thar margin. *Current Science* **84**, 1048-1055.

Juyal, N., Kar, A., Rajaguru, S. N. and Singhvi, A. K. (2003). Luminescence chronology of aeolian deposition during the Late Quaternary on the southern margin of Thar Desert, India. *Quaternary International* **104**, 87-98.

Kemp, R. A., Toms, P. S., Sayago, J. M., Derbyshire, E., King, M. and Wagoner, L. (2003). Micromorphology and OSL dating of the basal part of the loess-paleosol sequence at La Mesada in Tucuman province, Northwest Argentina. *Quaternary International* **106/107**, 111-117.

Kitis, G., Pagonis, V. and Drupieski, C. (2003). Cooling rate effects on the thermoluminescence glow curves of Arkansas quartz. *Physica Status Solidi A: Applied Research* **198**, 312-321.

Lahitte, P., Gillot, P. Y., Kidane, T., Courtillot, V. and Bekele, A. (2003). New age constraints on the timing of volcanism in central Afar, in the presence of propagating rifts. *Journal of Geophysical Research - Solid Earth* **108**, 2123.

Lang, A. (2003). Phases of soil erosion-derived colluviation in the loess hills of South Germany. *Catena* **51**, 209-221.

Malec-Czechowska, K., Strzelczak, G., Dancewicz, A. M., Stachowicz, W. and Delincee, H. (2003). Detection of irradiation treatment in dried mushrooms by photostimulated luminescence, EPR spectroscopy and thermoluminescence measurements. *European Food Research and Technology* **216**, 157-165.

Matmon, A., Crouvi, O., Enzel, Y., Bierman, P., Larsen, J., Porat, N., Amit, R. and Caffee, M. (2003). Complex exposure histories of chert clasts in the Late Pleistocene shorelines of Lake Lisan, southern Israel. *Earth Surface Processes and Landforms* **28**, 493-506.

Morgenstein, M. E., Luo, S., Lu, T. L. and Feathers, J. (2003). Uranium-series and luminescence dating of volcanic lithic artefacts. *Archaeometry* **45**, 503-518.

Nakagawa, T., Usuda, H. and Hashimoto, T. (2003). Optically stimulated luminescence (OSL) and thermoluminescence (TL) measurements on red TL (RTL) quartz samples using a new automated OSL/TL measuring system. *Journal of Radioanalytical and Nuclear Chemistry* **255**, 355-358.

Owen, L. A., Spencer, J. Q., Ma, H. Z., Barnard, P. L., Derbyshire, E., Finkel, R. C., Caffee, M. W. and Nian, Z. Y. (2003). Timing of Late Quaternary glaciation along the southwestern slopes of the Qilian Shan, Tibet. *Boreas* **32**, 281-291.

Pagonis, V., Kitis, G. and Chen, R. (2003). Applicability of the Zimmerman predose model in the thermoluminescence of predosed and annealed synthetic quartz samples. *Radiation Measurements* **37**, 267-274.

Personius, S. F. and Mahan, S. A. (2003). Paleoearthquakes and eolian-dominated fault sedimentation along the Hubbell Spring fault zone near Albuquerque, New Mexicao. *Bulletin of the Seismological Society of America* **93**, 1355-1369.

Poolton, N. R. J., Malins, A. E. R., Quinn, F. M., Pantos, E., Andersen, C. E., Bøtter-Jensen, L., Johnsen, O. and Murray, A. S. (2003). Luminescence excitation characteristics of Ca-, Na- and K-aluminosilicates (feldspars), in the stimulation range 20-500 eV; optical detection of XAS. *Journal of Physics D - Applied Physics* **36**, 1107-1114.

Preusser, F., Geyh, M. A. and Schlüchter, C. (2003). Timing of Late Pleistocene climate change in lowland Switzerland. *Quaternary Science Reviews* **22**, 1435-1445.

Rink, W. J. (2003). Thermoluminescence of quartz and feldspar sand grains as a tracer of nearshore environmental processes in the southeastern Mediterranean Sea. *Journal of Coastal Research* **19**, 723-730.

Rink, W. J., Bartoll, J., Goldberg, P. and Ronen, A. (2003). ESR dating of archaeologically relevant authigenic terrestrial apatite veins from Tabun Cave, Israel. *Journal of Archaeological Science* **30**, 1127-1138.

Roberts, H. M., Muhs, D. R., Wintle, A. G., Duller, G. A. T. and Bettis, E. A. (2003). Unprecedented last-glacial mass accumulation rates determined by luminescence dating of loess from western Nebraska. *Quaternary Research* **59**, 411-419.

Shaw, P. A., Bateman, M. D., Thomas, D. S. G. and Davies, F. (2003). Holocene fluctuations of Lake Ngami, Middle Kalahari: chronology and responses to climatic change. *Quaternary International* **111**, 23-35.

Singh, I. B., Jaiswal, M., Singhvi, A. K. and Singh, B. K. (2003). Rapid subsidence of western Ganga plain during late Pleistocene: evidence from optical dating of subsurface samples. *Current Science* **84**, 451-454.

Sørensen, R., Murray, A. S., Kaaya, A. K. and Kilasara, M. (2001). Stratigraphy and formation of a Late Pleistocene colluvial apron in Morogoro district, Central Tanzania. Palaeoecology of Africa and the surrounding islands. K. Heine and J. Runge, Balkema. **27,** 95-116.

Souza, S. O., Selvin, P. C. and Watanabe, S. (2003). Thermally stimulated luminescence, optical absorption and EPR studies on kyanite crystals. *Journal of Luminescence* **102**, 575-580.

Srivastava, P., Sharma, M. and Singhvi, A. K. (2003). Luminescence chronology of incision and channel pattern changes in the River Ganga, India. *Geomorphology* **51**, 259-268.

Srivastava, P., Singh, I. B., Sharma, M. and Singhvi, A. K. (2003). Luminescence chronometry and Late Quaternary geomorphic history of the Ganga Plain, India. *Palaeogeography, Palaeoclimatology , Palaeoecology* **197**, 15-41.

Srivastava, P., Singh, I. B., Sharma, S., Shukla, U. K. and Singhvi, A. K. (2003). Late Pleistocene-Holocene hydrologic changes in the interfluve areas of the central Ganga Plain, India. *Geomorphology* **54**, 279-292.

Stokes, S., Ingram, S., Aitken, M. J., Sirocko, F., Anderson, R. and Leuschner, D. (2003). Alternative chronologies for Late Quaternary (Last Interglacial-Holocene) deep sea sediments via optical dating of silt-sized quartz. *Quaternary Science Reviews* **22**, 925-941.

Sugio, K., Tatumi, S. H., Kowata, E. A., Munita, C. S. and Paiva, R. P. (2003). Upper Pleistocene deposits of the Comprida Island (Sao Paulo State) dated by thermoluminescence method. *Anais da Academia Brasiliera de Ciencias* **75**, 91-96.

Takano, M., Yawata, T. and Hashimoto, T. (2003). Luminescence dosimetry of archaeological and ceramic samples using a single-aliquot regenerative-dose method. *Journal of Radioanalytical and Nuclear Chemistry* **255**, 365-368.

Taranenko, V., Meckbach, R., Degteva, M. O., Bougrov, N. G., Göksu, Y., Vorobiova, M. I. and Jacob, P. (2003). Verification of external exposure assessment for the upper Techa riverside by luminescence measurement and Monte Carlo photon transport modeling. *Radiation and Environmental Biophysics* **42**, 17-26.

Tatumi, S. H., Kowata, E. A., Gozzi, G., Kassab, L. R. P., Suguio, K., Barreto, A. M. F. and Bezerra, F. H. R. (2003). Optical dating of beachrock, eolic dunes and sediments applied to sea-level changes study. *Journal of Luminescence* **102/103**, 562-565.

Tatumi, S. H., Peixoto, M. N. O., Moura, J. R. S., Mello, C. L., Carmo, I. O., Kowata, E. A., Yee, M., Brito, S. L. M., Gozzi, G. and Kassab, L. R. P. (2003). Optical dating using feldspar from Quaternary alluvial and colluvial sediments from SE Brazilian Plateau, Brazil. *Journal of Luminescence* **102/103**, 566-570.

Thomas, D. S. G., Brook, G., Shaw, P., Bateman, M., Haberyan, K., Appleton, C., Nash, D., McLaren, S. and Davies, F. (2003). Late Pleistocene wetting and drying in the NW Kalahari: an integrated study from the Tsodilo Hills, Botswana. *Quaternary International* **104**, 53067.

Thomas, M. F. and Murray, A. S. (2001). On the age and significance of Quaternary colluvium in eastern Zambia. Palaeoecology of Africa and the surrounding islands. K. H. a. J. Runge, Balkema. **27:** 117-133.

Trukhin, A., Kink, M., Maksimov, Y. and Kink, R. (2003). Self-trapped exciton luminescence in crystalline alpha-quartz under two-photon laser excitation. *Solid State Communications* **127**, 655-659.

Turkin, A. A., van Es, H. J., Vainshtein, D. I. and den Hartog, H. W. (2003). Thermoluminescence of zircon: a kinetic model. *Journal of Physics - Condensed Matter* **15**, 2875-2897.

Ujhazy, K., Gabris, G. and Frechen, M. (2003). Ages of periods of sand movement in Hungary determined through luminescence measurements. *Quaternary International* **111**, 91-100.

Vyas, P. R., Gandhi, Y. H. and Joshi, T. R. (2003). Effect of pre-thermal treatment on thermoluminescence of synthetic quartz. *Indian Journal of Pure and Applied Physics* **41**, 128-130.

Yazici, A. N. and Topaksu, M. (2003). The analysis of thermoluminescence glow peaks of unannealed synthetic quartz. *Journal of Physics D- Applied Physics* **36**, 620-627.

Part 2 : from 30 September 2003 to 31st March 2004

Bailey, R. M. (2003). Paper I: The use of measurement-time dependent single-aliquot equivalent-dose estimates from quartz in the identification of incomplete signal resetting. *Radiation Measurements* **37,** 673-683.

Bailey, R. M. (2003). Paper II: The interpretation of measurement-time dependent single-aliquot equivalent-dose estimates using predictions from a simple empirical model. *Radiation Measurements* **37,** 685-691.

Bailey, R. M. (2004). Paper I - simulation of dose absorption in quartz over geological timescales and its implications for the precision and accuracy of optical dating. *Radiation Measurements* **38,** 299-310.

Bailiff, I. K., and Mikhailik, V. B. (2004). The use of calcium silicate bricks for retrospective dosimetry. *Radiation Measurements* **38,** 91-99.

Bailiff, I. K., Stepanenko, V. F., Goksu, H. Y., Bøtter-Jensen, L., Brodski, L., Chumak, V., Correcher, V., Delgado, A., Golokov, V., Jungner, H., Khamidova, L. G., Kolizhenkov, T. V., Likhtarev, I., Meckbach, R., Petrov, S. A., and Sholom, S. (2004). Comparison of retrospective dosimetry with computational modeling in two highly contaminated settlements downwind of the Chernobyl NPP. *Health Physics* **86,** 25-41.

Baril, M. R. (2004). CCD imaging of the infra-red stimulated luminescence of feldspars. *Radiation Measurements* **38,** 81-86.

Baril, M. R. (2004). Emission and excitation spectra of feldspar inclusions within quartz. *Radiation Measurements* **38,** 87-90.

Baril, M. R., and Huntley, D. J. (2003). Infrared stimulated luminescence and phosphorescence spectra of irradiated feldspars. *Journal of Physics: Condensed Matter* **15,** 8029-8048.

Baril, M. R., and Huntley, D. J. (2003). Optical excitation spectra of trapped electrons in irradiated feldspars. *Journal of Physics: Condensed Matter* **15,** 8011-8027.

Bayram, G., and Delincee, H. (2004). Identification of irradiated Turkish foodstuffs combining various physical detection methods. *Food Control* **15,** 81-91.

Berger, G. W., Henderson, T. K., Banerjee, D., and Nials, F. L. (2004). Photonic dating of prehistoric irrigation canals at Phoenix, Arizona, USA. *Geoarchaeology* **19,** 1-19.

Bishop, P., Sanderson, D. C. W., and Stark, M. (2004). OSL and radiocarbon dating of a pre-Angkorian canal in the Mekong delta, southern Cambodia. *Journal of Archaeological Science* **31,** 319-336.

Blum, M. D., Carter, A. E., Zayac, T., and Goble, R. J. (2002). Middle Holocene sea-level and evolution of the Gulf of Mexico Coast (US). *Journal of Coastal Research* **36,** 65-80.

Bøtter-Jensen, L., McKeever, S. W. S., and Wintle, A. G. (2003). "Optically Stimulated Luminescence Dosimetry." Elsevier, Amsterdam.

Bowman, D., Korjertkov, A., and Porat, N. (2004). Late-Pleistocene seismites from Lake Issyk-Kul, the Tien Shan Range, Kyrghyzstan. *Sedimentary Geology* **163,** 211-228.

Bray, H. E., and Stokes, S. (2004). Temporal patterns of arid-humid transitions in the south-eastern Arabian Peninsula based on optical dating. *Geomorphology* **59,** 271-280.

Correcher, V., Garcia-Guinea, J., Sanchez-Munoz, L., and Delgado, A. (2003). Effect of dopants in the luminescence properties of synthetic quartz for dosimetric purposes. *Journal of Materials Processing Technology* **143,** 871-874.

Correcher, V., Garcia-Guinea, J., and Valle-Fuentes, F. J. (2003). Recent results on the thermoluminescence properties of diaspore. *Geophysical Research Letters* **30,** article 1949.

Correcher, V., Robredo, L. M., Valle-Fuentes, F. J., Lopez-Arce, P., and Garcia-Guinea, J. (2003). Characterization of the thermoluminescence curve of zircon by radioactive content and differential thermal analysis (in Spanish). *Boletin de la Sociedad Espanola de Ceramica y Vidrio* **42,** 369-373.

Crone, A. J., de Martini, P. M., Machette, M. N., Okumura, K., and Prescott, J. R. (2003). Paleoseismicity of two historically quiescent faults in Australia: implications for fault behavior in stable continental margins. *Bulletin of the Seismological Society of America* **93,** 1913-1934.

Despriee, J., and Gageonnet, R. (2003). The very high alluvial formation of early Pleistocene age in the Creuse River Valley at Eguzon (Indre): cryoturbation patterns, prehistoric occupation sites and absolute dating (in French). *Bulletin de la Societe Geologique de France* **174,** 383-400.

Duller, G. A. T. (2004). Luminescence dating of Quaternary sediments: recent advances. *Journal of Quaternary Science* **19,** 183-192.

Erfurt, G. (2003). Infrared luminescence of Pb+ centres in potassium-rich feldspars. *Physica Status Solidi A* **200,** 429-438.

Fattahi, M. (2004). The dependence of orange-red IRSL decay curves of potassium feldspars on sample temperature. *Radiation Measurements* **38,** 287-298.

Fattahi, M., and Stokes, S. (2003). Red luminescence from potassium feldspar for dating applications: a study of some properties relevant for dating. *Radiation Measurements* **37,** 647-660.

Fattahi, M., and Stokes, S. (2004). Absorbed dose evaluation in feldspar using a single-aliquot regenerative-dose (SAR) infrared-stimulated red luminescence protocol. *Radiation Measurements* **38,** 127-134.

Fiebig, M., Preusser, M., and Preusser, F. (2003). The age of fluvial sediments from the Ingolstadt area (Bavaria) and their significance for the stratigraphy of the ice age in the Alpine foreland. *Zeitschrift fur Geomorphologie* **47,** 449-467.

Forman, S. L., and Pierson, J. (2003). Formation of linear and parabolic dunes on the eastern Snake River Plain, Idaho in the nineteenth century. *Geomorphology* **56,** 189-200.

Frechen, M., Oches, E. A., and Kohfield, K. E. (2003). Loess in Europe - mass accumulation rates during the Last Glacial Period. *Quaternary Science Reviews* **22,** 1835-1857.

French, H. M., Demitroff, M., and Forman, S. L. (2003). Evidence for Late-Pleistocene permafrost in the New Jersey Pine Barrens (latitude 29 degrees N), eastern USA. *Permafrost and Periglacial Processes* **14,** 259-274.

Grün, R., Beaumont, P. B., Tobias, P. V., and Eggins, S. (2003). On the age of Border Cave 5 human mandible. *Journal of Human Evolution* **45,** 155-167.

Hashimoto, T. (2003). Basic and applied studies of radiation-induced luminescence from natural minerals (in Japanese). *Journal of the Atomic Energy Society of Japan* **45,** 497-501.

Henriksen, M., Mangerud, J., Matiouchkov, A., Paus, A., and Svendsen, J. I. (2003). Lake stratigraphy implies an 80 000 yr delayed melting of buried ice in northern Russia. *Journal of Quaternary Science* **18,** 663-679.

Hesse, P. P., Humphreys, G. S., Smith, B. L., Campbell, J., and Peterson, E. K. (2003). Age of loess deposits in the Central Tablelands of New South Wales. *Australian Journal of Soil Research* **41,** 1115-1131.

Hille, A., Junge, F. W., Geyh, M. A., Krbetschek, M., and Kremenetski, C. (2004). Characterising and dating Weichselian organogenic sediments: a case study from the Lusatian ice marginal valley (Scheibe opencast mine, eastern Germany). *Palaeogeography, Palaeoclimatology, Palaeoecology* **205,** 273-294.

Houmark-Nielsen, M., and Kjaer, K. H. (2003). Southwest Scandinavia, 40-15 kyr BP: palaeogeography and environmental change. *Journal of Quaternary Science* **18,** 769-786.

Huang, C. C., Pang, J. L., Chen, S. E., and Zhang, Z. P. (2003). Holocene dust accumulation and the formation of polycyclic cinnamon soils (luvisols) in the Chinese Loess Plateau. *Earth Surface Processes and Landforms* **28,** 1259-1270.

Jain, M., Bøtter-Jensen, L., and Singhvi, A. K. (2003). Dose evaluation using multiple-aliquot quartz OSL: test of methods and a new protocol for improved accuracy and precision. *Radiation Measurements* **37,** 67-80.

Jain, M., and Tandon, S. K. (2003). Fluvial response to Late Quaternary climate changes, western India. *Quaternary Science Reviews* **22,** 2223-2235.

Jain, M., Thomsen, K. J., Bøtter-Jensen, L., and Murray, A. S. (2004). Thermal transfer and apparent-dose distributions in poorly bleached mortar samples: results from single grains and small aliquots of quartz. *Radiation Measurements* **38,** 101-109.

Kamp, U. K., Haserodt, K., and Shroder, J. F. (2004). Quaternary landscape evolution in the eastern Hindu Kush, Pakistan. *Geomorphology* **57,** 1-27.

Kemp, R. A., P.S., T., King, M., and Krohling, D. M. (2004). The pedosedimentary evolution and chronology of Tortugas, a Late Quaternary type-site of the northern Pampa, Argentina. *Quaternary International* **114,** 101-112.

Kresten, P., Goedicke, C., and Manzano, A. (2004). TL-dating of vitrified material. *Geochronometria* **22,** 9-14.

Lang, A., Niller, H. P., and Rind, M. M. (2003). Land degradation in Bronze Age Germany: archaeological, pedological, and chronometrical evidence from a hilltop settlement on the Frauenberg, Niederbayern. *Geoarchaeology* **18,** 757-778.

Leigh, D. S., Srivastava, P., and Brook, G. A. (2004). Late Pleistocene braided rivers of the Atlantic coastal plain. *Quaternary Science Reviews* **23,** 65-84.

Lokrantz, H., Ingolfsson, O., and Forman, S. L. (2003). Glaciotectonised Quaternary sediments at Cape Shpindler, Yugorski Peninsula, Arctic Russia: implications for glacial history, ice movements and Kara Sea Ice Sheet configuration. *Journal of Quaternary Science* **18,** 527-543.

Mason, J. A., Jacobs, P. M., Hanson, P. R., Miao, X. D., and Goble, R. J. (2003). Sources and paleoclimatic significance of Holocene Bignell Loess, Central Great Plains, USA. *Quaternary Research* **60,** 330-339.

Mason, J. A., Swinehart, J. B., Goble, R. J., and Loope, D. B. (2004). Late-Holocene dune activity linked to hydrological drought, Nebraska Sand Hills, USA. *The Holocene* **14,** 209-217.

Mayer, J. H., and Mahan, S. A. (2004). Late Quaternary stratigraphy and geochronology of the western Killpecker Dunes, Wyoming, U.S.A. *Quaternary Research* **61,** 72-84.

McLaren, S. J., Gilbertson, D. D., Grattan, J. P., Hunt, C. O., Duller, G. A. T., and Barker, G. A. (2004). Quaternary Palaeogeomorphic evolution of the Wadi Faynan area, southern Jordan. *Palaeogeography, Palaeoclimatology, Palaeoecology* **205,** 131-154.

Mee, A. C., Bestland, E. A., and Spooner, N. A. (2004). Age and origin of Terra Rossa soils in the Coonawarra area of South Australia. *Geomorphology* **58,** 1-25.

Mercier, N., and Valladas, H. (2003). Reassessment of TL age estimates of burnt flints from the Paleolithic site of Tabun Cave, Israel. *Journal of Human Evolution* **45,** 401-409.

Miallier, D., Condomines, M., Pilleyre, T., Sanzelle, S., and Guittet, J. (2004). Concordant thermoluminescence and 238U-230Th ages for a trachytic dome (Grand Sarcoui) from the Chaine des Puys (French Massif Central). *Quaternary Science Reviews* **23,** 709-715.

Miallier, D., Sanzelle, S., Pilleyre, T., Vernet, G., Brugiere, S., and Danhara, T. (2004). Chronological and mineralogical data about the Sarlieve tephra and the CF7 tephra, chronostratigraphical marks in Grande Limagne (Massif Central, France) (in French). *Comptes Rendus Geoscience* **336,** 1-8.

Murton, J. B., Bateman, M. D., Baker, C. A., Knox, R., and Whiteman, C. A. (2003). The Devensian periglacial record on Thanet, Kent, UK. *Permafrost and Periglacial Processes* **14,** 217-246.

Ogundare, F. O., Balogun, F. A., and Hussain, L. A. (2004). Kinetic characterization of the thermoluminescence of natural fluorite. *Radiation Measurements* **38,** 281-286.

Otvos, E. G. (2004). Prospects for interregional correlations using Wisconsin and Holocene aridity episodes, northern Gulf of Mexico coastal plain. *Quaternary Research* **61,** 105-118.

Owen, L. A., Finkel, R. C., Haizhou, M., Spencer, J. Q., Derbyshire, E., Barnard, P. L., and Caffee, M. W. (2003). Timing and style of Late Quaternary glaciation in northeastern Tibet. *Geological Society of America Bulletin* **115,** 1356-1364.

Pan, B. T., Burbank, D., Wang, Y. X., Wu, G. J., Li, J. J., and Guan, Q. Y. (2003). A 900 ky record of strath terrace formation during glacial-interglacial transitions in northwest China. *Geology* **31,** 957-960.

Ponnusamy, V., Ramasamy, V., and Hemalatha, J. (2004). Thermostimulated luminescence (tsl) - thermal treatment in blue coloured calcite crystals. *Indian Journal of Pure and Applied Physics* **42,** 130-135.

Poolton, N. R. J., Bøtter-Jensen, L., Andersen, C. E., Jain, M., Murray, A. S., Malins, A. E. R., and Quinn, F. M. (2003). Measuring modulated luminescence using non-modulated stimulation: ramping the sample period. *Radiation Measurements* **37,** 639-645.

Porat, N., Wintle, A. G., and Ritte, M. (2004). Mode and timing of kurkar and hamra formation, central coastal plain, Israel. *Israel Journal of Earth Sciences* **53,** 13-25.

Prescott, J. R., Robertson, G. B., Shoemaker, C., Shoemaker, E. M., and Wynn, J. (2004). Luminescence dating of the Wabar meteorite craters, Saudi Arabia. *Journal of Geophysical Research-Planets* **109,** E01008.

Quinn, F., Poolton, N., Malins, A., Pantos, E., Andersen, C., CDenby, P., Dhanak, V., and Miller, G. (2003). The mobile luminescence end-station, MoLES: a new public facility at Daresbury Synchrotron. *Journal of Synchrotron Radiation* **10,** 461-466.

Raab, A., Melles, M., Berger, G. W., Hagedorn, B., and Hubberten, H. W. (2003). Non-glacial paleoenvironments and the extent of Weichselian ice sheets on Severnaya Zemlya, Russian High Arctic. *Quaternary Science Reviews* **22,** 2267-2283.

Richter, D. K., Gotte, T., Gotze, J., and Neuser, R. D. (2003). Progress in application of cathodoluminescence (CL) in sedimentary petrology. *Mineralogy and Petrology* **79,** 127-166.

Rink, W. J. (2003). Electron spin resonance and luminescent dating. *Physics in Canada* **59,** 269-274.

Rink, W. J., Schwarcz, H. P., Ronen, A., and Tsatskin, A. (2004). Confirmation of a near 400 ka age for the Yabrudian industry at Tabun Cave, Israel. *Journal of Archaeological Science* **31,** 15-20.

Roberts, H. M., and Duller, G. A. T. (2004). Standardised growth curves for optical dating of sediment using multiple-grain aliquots. *Radiation Measurements* **38,** 241-252.

Roberts, H. M., and Wintle, A. G. (2003). Luminescence sensitivity changes of polymineral fine grains during IRSL and [post-IR] OSL measurements. *Radiation Measurements* **37,** 661-671.

Roque, C., Guibert, P., Vartanian, E., Viellevigne, E., and Bechtel, F. (2004). Changes in luminescence properties induced by thermal treatments: a case study at Sipan and Trujillo Moche sites (Peru). *Radiation Measurements* **38,** 119-126.

Sakurai, T., and Gartia, R. K. (2003). Method of computerized glow curve deconvolution for analysing thermoluminescence. *Journal of Physics D - Applied Physics* **36,** 2719-2724.

Sanderson, D. C. W., Carmichael, L. A., and Fisk, S. (2003). Photostimulated luminescence detection of irradiated herbs, spices, and seasonings: international interlaboratory trial. *Journal of AOAC International* **86,** 990-997.

Sanderson, D. C. W., Carmichael, L. A., and Fisk, S. (2003). Photostimulated luminescence detection of irradiated shellfish: international interlaboratory trial. *Journal of AOAC International* **86,** 983-989.

Sanderson, D. C. W., Carmichael, L. A., and Fisk, S. (2003). Thermoluminescence detection of irradiated fruits and vegetables: international interlaboratory trial. *Journal of AOAC International* **86,** 971-975.

Sanderson, D. C. W., Carmichael, L. A., and Fisk, S. (2003). Thermoluminescence detection of irradiated shellfish: international interlaboratory trial. *Journal of AOAC International* **86,** 976-982.

Sastry, M. D., Sullasi, H. S. L., Camargo, F., Watanabe, S., Prous, A. P. P., and Silva, M. M. C. (2004). Dating sediment deposits on Montalvanian carvings using EPR and TL methods. *Nuclear Instruments and Methods in Physics Research B* **213,** 751-755.

Schellmann, G., and Radtke, U. (2004). A revised morpho- and chronostratigraphy of the Late and Middle Pleistocene coral reef terraces on Southern Barbados (West Indies). *Earth Science Reviews* **64,** 157-187.

Schokker, J., Cleveringa, P., and Murray, A. S. (2004). Palaeoenvironmental reconstruction and OSL dating of terrestrial Eemian deposits in the southeastern Netherlands. *Journal of Quaternary Science* **19,** 193-202.

Sekkina, M. A., El Fiki, M. A., Nossair, S. A., and Khalil, N. R. (2003). Thermoluminescence archaeological dating of pottery in the Egyptian pyramids zone. *Ceramics-Silikaty* **47,** 94-99.

Singarayer, J. S., and Bailey, R. M. (2004). Component-resolved bleaching spectra of quartz optically stimulated luminescence: preliminary results and implications for dating. *Radiation Measurements* **38,** 111-118.

Soliman, C. (2003). Some luminescence properties of the blue emission band of muscovite. *Radiation Effects and Defects in Solids* **158,** 667-673.

Spencer, J. Q., and Owen, L. A. (2004). Optically stimulated luminescence dating of Late Quaternary glaciogenic sediments in the upper Hunza valley: validating the timing of glaciation and assessing dating methods. *Quaternary Science Reviews* **23,** 175-191.

Stokes, S., Bailey, R. M., Fedoroff, N., and O'Marah, K. E. (2004). Optical dating of aeolian dynamism on the West African Sahelian margin. *Geomorphology* **59,** 281-291.

Stone, T., and Cupper, M. L. (2003). Last Glacial Maximum ages for robust humans at Kow Swamp, southern Australia. *Journal of Human Evolution* **45,** 99-111.

Sullasi, H. S., Andrade, M. B., Ayta, W. E. F., Frade, M., Sastry, M. D., and Watanabe, S. (2004). Irradiation for dating Brazilian fish fossil by thermoluminescence and EPR technique. *Nuclear Instruments and Methods in Physics Research B* **213,** 756-760.

Teeuw, R. M., and Rhodes, E. J. (2004). Aeolian activity in northern Amazonia: optical dating of Late Pleistocene and Holocene palaeodunes. *Journal of Quaternary Science* **19,** 49-54.

Truelsen, J. L., and Wallinga, J. (2004). Zeroing of the OSL signal as a function of grain size: investigating bleaching and thermal transfer for a young fluvial sample. *Geochronometria* **22,** 1-8.

Trukhin, A., and Poumellec, B. (2004). Energy transport in silica to oxygen-deficient luminescence centers: comparison with other luminescence centers in silica and alpha-quartz. *Solid State Communications* **129,** 285-289.

Ulusoy, U. (2004). ESR dating of North Anatolian (Turkey) and Nojima (Japan) faults. *Quaternary Science Reviews* **23,** 161-174.

Valladas, H., Mercier, N., Joron, J. L., McPherron, S. P., Dibble, H. L., and Lenoir, M. (2003). TL dates for the Middle Paleolithic site of Combe-Capelle Bas, France. *Journal of Archaeological Science* **30,** 1443-1450.

Van Peer, P., Fullagar, R., Stokes, S., Bailey, R. M., Moeyersons, J., Steenhoudt, F., Geerts, A., Vanderbeken, T., De Dapper, M., and Geus, F. (2003). The Early to Middle Stone Age transition and the emergence of modern human behaviour at site 8-B-11, Sai Island, Sudan. *Journal of Human Evolution* **45,** 187-193.

Vandenberghe, D., Kasse, C., Hossain, S. M., de Corte, F., van den Haute, P., Fuchs, M., and Murray, A. S. (2004). Exploring the method of optical dating and comparison of optical and 14C ages of Late Weichselian coversands in the southern Netherlands. *Journal of Quaternary Science* **19,** 73-86.

Vyas, P. R., and Joshi, T. R. (2003). Some thermoluminescence properties of synthetic quartz and its potential as high level gamma radiation thermoluminescence dosimeter material. *Indian Journal of Physics and Proceedings of the Indian Association for the Cultivation of Science* **77A,** 285-287.

Williams, M. A. J., Adamson, D., Prescott, J. R., and Williams, F. M. (2003). New light on the age of the White Nile. *Geology* **31,** 1001-1004.

Yamaguchi, T., Mitamura, N., Takeuchi, A., and Hashimoto, T. (2003). Changes of luminescence properties dependent on OH-impurities in natural quartz (in Japanese). *Bunseki Kagaku* **52,** 787-793.

Yordanov, N. D., and Aleksieva, K. (2004). X- and Q-band EPR studies on fine powders of irradiated plants. New approach for detection of their radiation history by using Q-band EPR spectrometry. *Radiation Physics and Chemistry* **69,** 59-64.

Part 3: Papers from Reno LED02 volume of Radiation Measurements in alphabetical order

Andersen, C. E., Bøtter-Jensen, L. and Murray, A. S. (2003). A mini X-ray generator as an alternative to a Sr-90/Y-90 beta source in luminescence dating. *Radiation Measurements* **37**, 557-561.

Auclair, M., Lamothe, M. and Huot, S. (2003). Measurement of anomalous fading for feldspar IRSL using SAR. *Radiation Measurements* **37**, 487-492.

Aznar, M. C., Nathan, R., Murray, A. S. and Bøtter-Jensen, L. (2003). Determination of differential dose rates in a mixed beta and gamma field using shielded Al2O3 : C: results of Monte Carlo modelling. *Radiation Measurements* **37**, 329-334.

Bailey, R. M., Singarayer, J. S., Ward, S. and Stokes, S. (2003). Identification of partial resetting using D-e as a function of illumination time. *Radiation Measurements* **37**, 511-518.

Bortolot, V. J. and Bluszcz, A. (2003). Strategies for flexibility in luminescence dating: procedure- oriented measurement and hardware modularity. *Radiation Measurements* **37**, 551-555.

Bøtter-Jensen, L., Andersen, C. E., Duller, G. A. T. and Murray, A. S. (2003). Developments in radiation, stimulation and observation facilities in luminescence measurements. *Radiation Measurements* **37**, 535-541.

Brennan, B. J. (2003). Beta doses to spherical grains. *Radiation Measurements* **37**, 299-303.

Burbidge, C. I. and Duller, G. A. T. (2003). Combined gamma and beta dosimetry, using Al2O3 : C, for in situ measurements on a sequence of archaeological deposits. *Radiation Measurements* **37**, 285-291.

Chen, R. and Leung, P. L. (2003). The decay of OSL signals as stretched-exponential functions. *Radiation Measurements* **37**, 519-526.

Chithambo, M. L. (2003). The influence of annealing and partial bleaching on luminescence lifetimes in quartz. *Radiation Measurements* **37**, 467-472.

Duller, G. A. T., Bøtter-Jensen, L. and Murray, A. S. (2003). Combining infrared- and green-laser stimulation sources in single-grain luminescence measurements of feldspar and quartz. *Radiation Measurements* **37**, 543-550.

Erfurt, G. and Krbetschek, M. R. (2003). Studies on the physics of the infrared radioluminescence of potassium feldspar and on the methodology of its application to sediment dating. *Radiation Measurements* **37**, 505-510.

Garcia-Guinea, J., Correcher, V., Delgado, A. and Sanchez-Munoz, L. (2003). Cluster linkages between luminescence emission spectra and continuous trap distribution in a volcanic sanidine. *Radiation Measurements* **37**, 473-477.

Goedicke, C. (2003). Dating historical calcite mortar by blue OSL: results from known age samples. *Radiation Measurements* **37**, 409-415.

Göksu, H. Y., Bailiff, I. K. and Mikhailik, V. B. (2003). New approaches to retrospective dosimetry using cementitious building materials. *Radiation Measurements* **37**, 323-327.

Hashimoto, T., Yamaguchi, T., Fujita, H. and Yanagawa, Y. (2003). Comparison of infrared spectrometric characteristics of Al-OH impurities and thermoluminescence patterns in natural quartz slices at temperatures below 0 degrees C. *Radiation Measurements* **37**, 479-485.

Huot, S. and Lamothe, M. (2003). Variability of infrared stimulated luminescence properties from fractured feldspar grains. *Radiation Measurements* **37**, 499-503.

Jain, M., Murray, A. S. and Bøtter-Jensen, L. (2003). Characterisation of blue-light stimulated luminescence components in different quartz samples: implications for dose measurement. *Radiation Measurements* **37**, 441-449.

Kalchgruber, R., Fuchs, M., Murray, A. S. and Wagner, G. A. (2003). Evaluating dose-rate distributions in natural sediments using alpha-Al2O3 : C grains. *Radiation Measurements* **37**, 293-297.

Khan, R. F. H., Rink, W. J. and Boreham, D. R. (2003). Dosimetric response evaluation of tooth enamel for accelerator- based neutron radiation. *Radiation Measurements* **37**, 355-363.

Lamothe, M., Auclair, M., Hamzaoui, C. and Huot, S. (2003). Towards a prediction of long-term anomalous fading of feldspar IRSL. *Radiation Measurements* **37**, 493-498.

Matsuda, T., Yamanaka, C. and Ikeya, M. (2003). Adsorption of Gd3+ into sediments: simulation of actinide adsorption on a clay mineral and hydroxyapatite. *Radiation Measurements* **37**, 371-375.

McKeever, S. W. S., Banerjee, D., Blair, M., Clifford, S. M., Clowdsley, M. S., Kim, S. S., Lamothe, M., Lepper, K., Leuschen, M., McKeever, K. J., Prather, M., Rowland, A., Reust, D., Sears, D. W. G. and Wilson, J. W. (2003). Concepts and approaches to in situ luminescence dating of martian sediments. *Radiation Measurements* **37**, 527-534.

Murray, A. S. and Wintle, A. G. (2003). The single aliquot regenerative dose protocol: potential for improvements in reliability. *Radiation Measurements* **37**, 377-381.

Nakagawa, T. and Hashimoto, T. (2003). Sensitivity change of OSL and RTL signal from natural RTL quartz with annealing treatment. *Radiation Measurements* **37**, 397-400.

Nathan, R. P., Thomas, P. J., Jain, M., Murray, A. S. and Rhodes, E. J. (2003). Environmental dose rate heterogeneity of beta radiation and its implications for luminescence dating: Monte Carlo modelling and experimental validation. *Radiation Measurements* **37**, 305-313.

Sato, H., Yamanaka, C. and Ikeya, M. (2003). Basic study on electrically stimulated luminescence (ESL) as a dosimetry and dating method. *Radiation Measurements* **37**, 335-339.

Sholom, S. V. and Chumak, V. V. (2003). Decomposition of spectra in EPR dosimetry using the matrix method. *Radiation Measurements* **37**, 365-370.

Singarayer, J. S. and Bailey, R. M. (2003). Further investigations of the quartz optically stimulated luminescence components using linear modulation. *Radiation Measurements* **37**, 451-458.

Spencer, J. Q., Sanderson, D. C. W., Deckers, K. and Sommerville, A. A. (2003). Assessing mixed dose distributions in young sediments identified using small aliquots and a simple two-step SAR procedure: the F-statistic as a diagnostic tool. *Radiation Measurements* **37**, 425-431.

Stokes, S. and Fattahi, M. (2003). Red emission luminescence from quartz and feldspar for dating applications: an overview. *Radiation Measurements* **37**, 383-395.

Thomsen, K. J., Jain, M., Bøtter-Jensen, L., Murray, A. S. and Jungner, H. (2003). Variation with depth of dose distributions in single grains of quartz extracted from an irradiated concrete block. *Radiation Measurements* **37**, 315-321.

Toyoda, S., Tanizawa, H., Romanyukha, A. A., Miyazawa, C., Hoshi, M., Ueda, Y. and Nitta, Y. (2003). Gamma-ray dose response of ESR signals in tooth enamel of cows and mice in comparison with human teeth. *Radiation Measurements* **37**, 341-346.

Tsukamoto, S., Rink, W. J. and Watanuki, T. (2003). OSL of tephric loess and volcanic quartz in Japan and an alternative procedure for estimating D-e from a fast OSL component. *Radiation Measurements* **37**, 459-465.

Vandenberghe, D., Hossain, S. M., De Corte, F. and Van den haute, P. (2003). Investigations on the origin of the equivalent dose distribution in a Dutch coversand. *Radiation Measurements* **37**, 433-439.

Ward, S., Stokes, S., Bailey, R., Singarayer, J., Goudie, A. and Bray, H. (2003). Optical dating of quartz from young samples and the effects of pre-heat temperature. *Radiation Measurements* **37**, 401-407.

Zdravkova, M., Wieser, A., El-Faramawy, N., Ivanov, D., Gallez, B. and Debuyst, R. (2003). An in vitro L-band EPR study with whole human teeth in a surface coil resonator. *Radiation Measurements* **37**, 347-353.

Zhao, H., Li, S. H. and Murray, A. S. (2003). Comparison of SAAD and SAR procedures for equivalent dose determination using quartz. *Radiation Measurements* **37**, 417-424.

News of the community

Martin Aitken

Doctoris Honoris Causa of the University Blaise Pascal (Clermont-Ferrand, France, 15 October 2003)

Introductory talk by Jean Faïn

J. F M.A.

I am honoured to present Professor Martin Aitken as Doctoris Honoris Causa of the University Blaise Pascal.

His initial career was in Nuclear Physics following a first degree in Physics at Oxford University. After completing his D.Phil. in 1954 and several years of research using an electron synchrotron he interested himself in applications of magnetism to archaeology especially in the use of a portable proton magnetometer for detecting buried pottery kilns and other archaeological remains.

In 1957 MA became Deputy Director of the Research Laboratory for Archaeology and the History of Art (RLAHA), Oxford, a position he held until his retirement in 1989. The aims of this laboratory focussed on applications of 'hard sciences' to archaeology following the recent emergence of radiocarbon dating. The word 'Archaeometry' was coined as the title for this activity jointly by MA and the then professor of archaeology at Oxford, Christopher Hawkes; it was also to become the title of a periodical that was launched by MA in 1958 which is to-day essential study for all those who work in the field.

At the beginning of the sixties MA involved himself and his students in the development of thermoluminescence dating (TL), in the first place in application to pottery; this had been tried unsuccessfully by a physicist in California a year or two before. Notably he found a way of suppressing 'spurious TL' and after taking account of radiation dosimetry the first actual dating results were published in the journal Nature in 1968. This new absolute technique eventually showed itself to be highly fruitful and during the seventies it was applied to a number of different approaches adapted to various situations. The Oxford Laboratory was the seedbed for a number of researchers who then started their own teams not only in UK but also in Europe, Australia, north America, India and elsewhere. In 1978 the first international congress on TL dating took place at Oxford; thereafter it became a regular meeting every two, then three years at various laboratories around the world, including also the technique of ESR dating with which it had the common concern of radiation dosimetry.

In 1978 the Oxford Laboratory successfully applied the TL technique to dating volcanic events; this was in collaboration with vulcanologists from the University Blaise Pascal as well as Norbert Bonhommet from Rennes. An age of 26000 years was obtained for sediments heated by the lava flow at Royat and 8500 years for the lava flow at St.Saturnin, both near to Clermont Ferrand; later more direct application to various lava flows was shown to be possible by Georges Valladas, Pierre-Yves Gillot and Gilles Guérin at the CEA-CNRS laboratory at Gif-sur-Yvette.

In the meantime Russian researchers showed that TL dating could be extended to windblown sediments and this was followed by the Simon Fraser laboratory in Canada which showed that the event dated was the last exposure of the sediment to sunlight; this laboratory also invented the associated technique of Optically Stimulated Luminescence (OSL) giving rise to a new domain of application which literally exploded during the eighties. All of this stemmed from the initial work at MA's Oxford Laboratory; at the same time MA devoted much effort to studies in archeomagnetism and palaeomagnetism and this was in part the stimulation for his visits to the Auvergne.

In 1980 a research group at the Laboratoire de Physique Corpusculaire of the University Blaise Pascal, which had previously acquired some expertise in application of TL to physics, began to use the method for dating. Very rapidly contacts, then collaborations, were linked to the Oxford Laboratory; I do indeed remember my visits to the laboratory, at 6 Keble Road, which was housed in a

domestic house rather than a purpose-built laboratory; access to the four floors was by means of crooked stairs which became more tortuous with increasing altitude! However I have mainly the memory of the warm and enriching welcome that we always received from Martin, his colleagues and students.

In the years following, collaboration with the RLAHA were extensive as, for example, on the controversial site of Glozel where Oxford carried on the important work initiated by the late Vagn Mejdahl in Denmark; there was also mutual participation in the examination of doctoral theses. During the international meeting at Cambridge in 1987 MA suggested that the next could be held in Clermont-Ferrand and this took place in 1990. MA is also a member of the Editorial Board of the international newsletter Ancient TL which is presently edited by the Clermont TL group following its founding in St.Louis by the late David Zimmerman and subsequent editing at Durham (UK).

Promoted Professor of Archaeometry at Oxford University in 1985 MA is also the author of several scientific books devoted to dating techniques especially that on TL dating, which is still the 'bible' in the field. He was honoured for his scientific achievements by the Gemant Award of the American Physical Institute and the award of the Pomerance Medal of the Archaeological Institute of America. In April last year on the occasion of his 80th birthday friends and colleagues of Martin gathered together in Clermont-Ferrand for a very interesting two days of scientific discussion.

Martin and his wife Joan have visited France many times over the course of years, interesting themselves particularly in local vineyards, and they finally decided to retire in the middle mountains not far from Clermont; we are very proud and honoured by this choice. I shall not forget to associate Madame Aitken with this ceremony; alas her state of health does not permit her attendance. Thus not only do we welcome in Clermont to-day, at the Université Blaise Pascal, a well-known researcher but also someone who is deeply attached to our region.

Meeting announcement

We would like to announce the **3rd New World Luminescence Dating Workshop**, which will take place at Dalhousie University, Halifax, Nova Scotia, Canada, 4 to 7th of July, 2004. The meeting should be of interest to luminescence dating specialists, geomorphologists, Quaternary geologists, archaeologists, and museum researchers. We are currently seeking funding to offset partial travel costs for students presenting papers.

Interested parties should contact the technical co-host, Mrs. P. Scallion, pscallio@dal.ca, with a request to be added to the mailing list for the first call for abstracts, which will be sent before the end of 2003.

Please forward this message to others who may find it of interest, with apologies for any future cross-listings.